Seasonal Hydrogen Storage in Depleted Gas Reservoirs

A Feasibility Study for The Netherlands

by

Thomas M.R.B. Visser

To obtain the degree of Master of Science in:
Petroleum Engineering and Geosciences
Faculty of Civil Engineering and Geosciences,
Delft University of Technology

To be defended publicly on Friday October 9, 2020 at 15:00.

Student number:	4294904	
Project duration:	November, 2019 – October, 2020	
Thesis committee:	Dr. H. Hajibeygi,	TU Delft, Supervisor and Committee Chair
	M. C.B. Robledo,	Ministry of Economic Affairs & Climate
	Dr. P.J. Vardon,	TU Delft
	Dr. Ir. D.S. Draganov,	TU Delft

This thesis is confidential and cannot be made public until October 9, 2020.

TU Delft

Acknowledgement

With this thesis I am finishing my MSc. Petroleum Engineering at the Delft University of Technology. Therefore, I would like to thank several people who have had a great contribution to this project.

First of all, I would like thank Dr. Hadi Hajibeygi for the inspirational lectures and courses throughout the MSc. program encouraging me to do further research in the field of subsurface hydrogen storage. The frequent meetings and discussions regarding this topic have been of enormous value throughout the project.

Secondly, I would like to thank Carla Robledo and the hydrogen team of the Dutch Ministry of Economic Affairs & Climate. Even though I performed the majority of the internship while working from home, I feel that I got a great overview of the activities of the Ministry and I am grateful for the experience that it is given to me.

Then, I would like to thank both PhD candidate Moussa HosseiniMehr and research assistant Leila Hashemi for their huge amount of help throughout this project. I would like to thank Moussa especially for all the help and challenges with the DARSim2 simulator and Leila for the fruitful collaboration regarding the topic of hydrogen storage in porous media and her supervising role in the hydrogen storage research group within DARSim.

Lastly, I would like to thank my friends, roommates, studymates, family and my girlfriend who have continuously supported throughout this project. The many conversations about the progress and issues while conducting the graduation project and all the (virtual) coffee breaks, lunches and laughs have helped enormously to stay motivated while working from home during the COVID-19 crisis.

Thomas M.R.B. Visser
Delft, October 2020

Abstract

The Netherlands will need to transform her traditionally fossil fueled energy system in the coming decades to achieve the goal of reducing CO_2 emissions to net-zero in 2050. Therefore, an increase in renewable energy sources as solar and wind energy in the overall energy mix will be essential. However, due to the highly variable energy production patterns of these renewable energy sources, a primary need for energy storage is created. Since electricity can not be stored on a large enough scale to balance significant energy fluctuations, the need for a gaseous CO_2 neutral energy carrier is created. In The Netherlands, this role could potentially be fulfilled by green hydrogen gas. Green hydrogen can be stored in geological formations such as depleted gas reservoirs. Due to the immense storage volumes and frequent occurrence in the Dutch subsurface, depleted gas reservoirs could be an excellent opportunity to serve as large scale energy storage sites. Moreover, underground natural gas storage in gas reservoirs is a proven and used technique in The Netherlands.

Utilizing a natural gas reservoir as a hydrogen storage site comes with several challenges. This report provides a full overview of all the challenges with underground hydrogen storage in geological formations as aquifers, depleted gas reservoirs and salt caverns based on literature. In this way, the full potential and risks of using depleted gas reservoirs for this technique is clearly highlighted. Using this overview, a priority scheme for the usage of different geological formations as storage facilities for hydrogen is proposed. In combination with possible meteorological conditions combined with different Dutch policy scenarios, a minimum seasonal storage need of 16 TWh through the use of hydrogen is identified. Using the priority scheme, rock salt caverns are used as much as possible to fulfill the minimal need for seasonal hydrogen storage. By performing an analysis on the potential subsurface storage capacity in The Netherlands, it becomes clear that the Dutch subsurface can not realize more than 12.1 TWh of potential hydrogen storage capacity by only utilizing salt caverns. Since depleted gas reservoirs are identified as the best alternative for underground hydrogen storage, a minimum need for hydrogen storage from Dutch depleted gas reservoirs is estimated at 3.9 TWh in 2050.

In this thesis, all physical and chemical aspects that are important during the subsurface storage of hydrogen in porous media are addressed. This leads to the identification of potential losses of hydrogen during the storage of the gas in the depleted gas reservoir. Analyzing all the possible methods leading to potential hydrogen loss shows that on the long term, bacterial conversion seems to be the biggest challenge if no measures against this conversion are taken.

Using numerical reservoir simulation as a quantification and sensitivity analysis tool, the hydrodynamic behaviour of hydrogen in contact with other gasses is described. This is done by introducing a dimensionless gravity number. The interpretation of this number shows if the displacement process is either dominated by viscous or gravitational forces. Furthermore, the displacement efficiency of hydrogen towards other gasses is analyzed. Displacement of hydrogen towards residual gasses in porous media dominated by viscous forces proves to be more efficient than the displacement dominated by gravitational forces.
By performing cyclic storage simulations, the overall efficiency of injecting and reproducing hydrogen from a depleted gas reservoir is examined. This is done for both homogeneous and heterogeneous reservoirs. By performing a sensitivity analysis on the input parameters of the simulator, an overview is given of the parameters that will have the most positive or negative impact on the cycle efficiency. The results of the simulation show a regular cycle efficiency that is estimated at roughly 70%. Applying a higher difference in injection and production pressure leads to a lower cycle efficiency whereas using a more elongate reservoir as storage site shows to have a positive effect on the overall cyclic efficiency.

Contents

List of Figures

List of Tables

1

Introduction

The Dutch Climate Agreement forces The Netherlands to reduce her emissions of greenhouses gas emission with 49% in 2030 [1]. Therefore, The Netherlands is facing a great challenge to adapt her national energy system. Traditional fossil fuels as coal, oil and gas need to be phased out throughout the coming decades and be substituted by CO_2 neutral energy sources. A current disadvantage of an energy mix dominated by renewable energy sources as solar and wind energy is the fact that these sources are fluctuating due to weather conditions causing intermittent electricity to be delivered to the grid [2]. Consequently, these fluctuations in energy production will cause surpluses and deficits and will therefore lead to an unreliable supply of energy. This mismatch of supply and demand for CO_2 neutral energy sources leads to a primary need for energy storage in the future.
Currently, renewable energy sources as solar and wind energy primarily produce electricity.

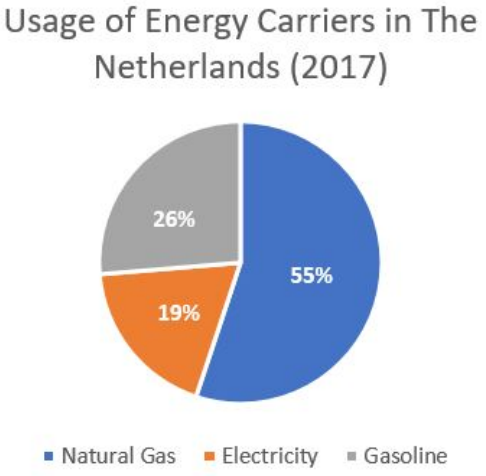

Figure 1.0.1: Used energy carriers in The Netherlands in 2017 [3]

Figure 1.0.1 shows that electricity only accounts for a relatively small share in the overall usage of energy carriers in The Netherlands [3]. Energy consuming sectors such as the industry and mobility will not be able to completely switch to electricity in the nearby future. In terms of potential, H_2 can also replace the energy carrying role for nearly 60% of non-industrial processes for which currently natural gas is used [4]. Moreover, the scale of electricity generation will not be great enough in order to supply each energy consuming sector with electricity [5]. Also, current storage technologies are limited in both capacity and discharge time when it comes to the storage of electricity [3]. Therefore, a primary demand for alternative energy carriers other than electricity will remain, for example through the use of 'green' gas (CH_4) or hydrogen gas (H_2). A great theoretical volume can be used as a storage site in which a clean energy carrier as H_2 can be stored. Through the use of large scale energy storage, fluctuations in energy usage and production can be balanced. In Figure 1.0.2 it is clear to see that energy storage through the use of hydrogen can be realized at a much greater scale than many other conventional storage techniques [6].

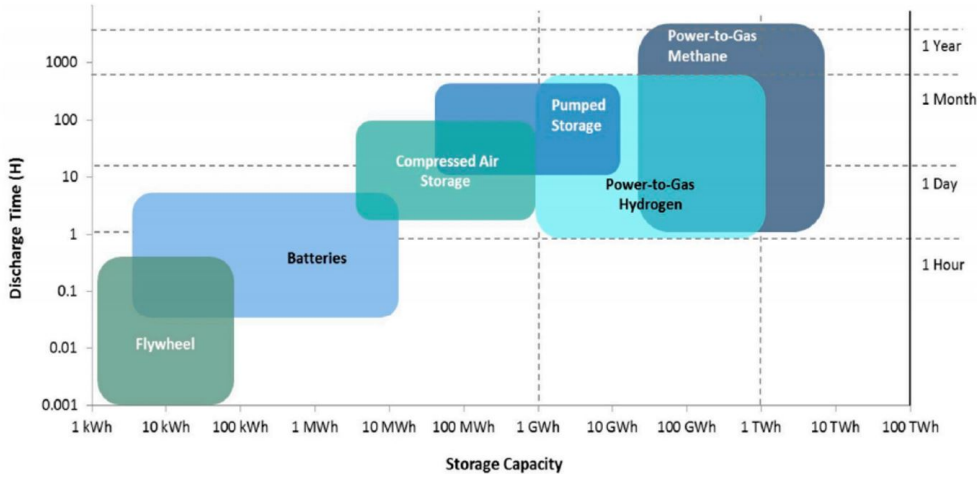

Figure 1.0.2: Discharge time vs. storage capacity for different storage technologies [6]

1.1. Hydrogen as an energy carrier and storage medium

Hydrogen (H) is the lightest and most abundant element that can be found on Earth [7]. The atom is largely present in a great amount of molecules like for example water (H_2O), methane (CH_4) and ammonia (NH_3). Pure hydrogen gas (H_2) however is not a natural source and needs to be produced through the use of different chemical reactions. The four biggest sources through which H_2 can be produced are coal, natural gas, oil and water. Currently, H_2 is mainly produced for industrial purposes using fossil fuels as a source. The most common method used nowadays is Steam-Methane-Reforming (SMR). In this process, H_2 is separated from CH_4 using high temperature steam [8], i.e.,

$$CH_4 + H_2O \rightarrow 3H_2 + CO. \tag{1.1}$$

Then, using the water-gas-shift reaction (WGSR), the produced carbon-monoxide CO is used for the following reaction producing again H_2, i.e.,

$$H_2O + CO \rightarrow H_2 + CO_2. \tag{1.2}$$

However, when applying SMR and WGSR to produce H_2, CO_2 is produced simultaneously which means that this production method for H_2 is not feasible due to the simultaneous production of greenhouse gas emissions. This process is therefore often referred to as grey H_2 production [9]. If, however, the produced CO_2 is then sequestrated and stored safely, no additional CO_2 will enter the atmosphere. This would mean a production of net CO_2 neutral H_2 which is often referred to as 'blue' H_2 production [9].

The production of green H_2 can be performed by several methods, including biomass induced processes and several water splitting techniques. The water splitting techniques include promising proton-exchange-membrane (PEM) water electrolysis through which 80-90% efficiency can be achieved [10]. When green electricity is used as the energy source for this process, green H_2 can be produced through the following chemical reaction:

$$2H_2O \rightarrow 2H_2 + O_2 \tag{1.3}$$

In this process, no carbon emission is established creating a carbon neutral methodology to produce the energy carrier H_2.

In the current energy infrastructure, oil and gas have the great benefit that these sources can be characterized as both natural resources and energy carriers. This means that both sources are relatively efficient to be produced, transported and consumed for different applications. Current green energy sources as solar and wind produce electricity as primary product which is not seen as an ideal energy carrier due to the limited capacity on the electricity grid and the inability to store large amounts of energy in batteries [3].
In order to replace the energy carrying role of an energy source like oil or natural gas, H_2 is a potential candidate to replace these fossil fuels. This is mainly due to the high energy density of H_2 making it a suitable energy carrier. As stated before, energy consuming processes are needed prior to production of H_2. Therefore it can only be seen as an energy carrier instead of an energy source.

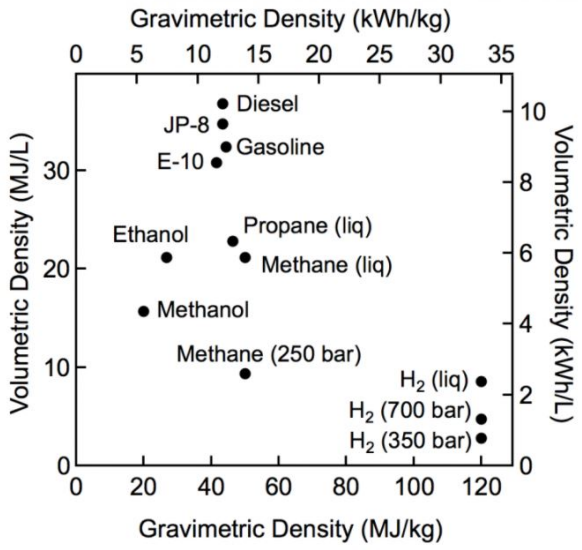

Figure 1.1.1: Volumetric and Gravimetric Density of several energy carriers [11]

In Figure (1.1.1) it is noticeable that the potential of H_2 can be found in the gravimetric density [11]. Therefore, in order to store the most energy in a volumetric unit, compression of H_2 is an essential step to be taken.

1.2. Seasonal energy storage

Another reason making H_2 a potential candidate for the future energy infrastructure can be found when looking at the relationship between energy consumption and production. The current usage of electricity and (industrial) gas are characterized by respectively small daily and large seasonal fluctuations. In The Netherlands, this difference is clearly visualized in the figure below:

The large difference in usage of natural gas is related to the demand for heat during the winter. This extra demand for gas can be compensated for by simply increasing the gas production rate from existing gas reservoirs or by making use of seasonal underground gas storage (UGS). Currently in The Netherlands, cheap gas is stored during the summer in four depleted onshore gas reservoirs. When heat demand rises in the winter, the stored gas is produced from these gas reservoirs completing the seasonal gas storage cycle. If in the future, H_2 would become the energy carrier for a large portion of the utilities for which now natural gas is used, the demand for H_2 would roughly follow the same seasonal demand curve.

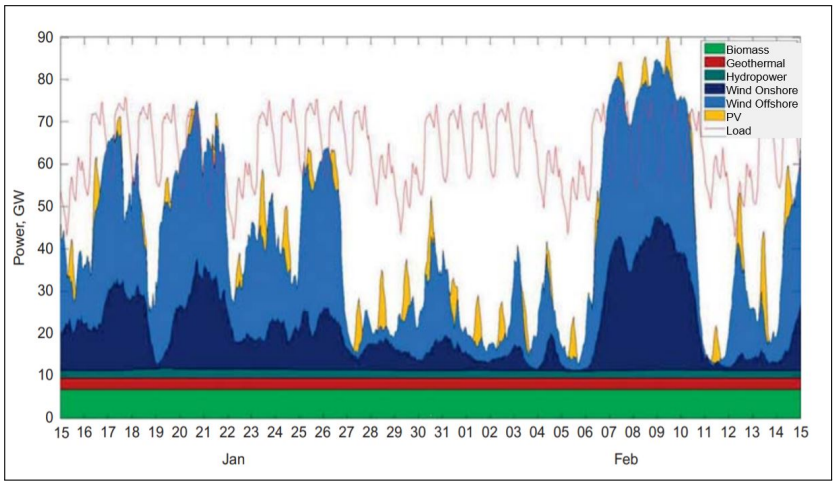

Figure 1.2.1: Fluctuations of Renewable Energy Production in Germany [17]

As mentioned before, if the future energy mix will rely on a great share of fluctuating renewable energy sources, the supply of energy will show both surpluses and deficits. In the above Figure(1.2.1), the typical scale of such fluctuations in the German energy mix are visualized throughout the months of January and February. The red line visualizes the load that is delivered to the electricity grid. During the last week of January and the first week of February, there is clearly not enough energy produced by renewable energy sources to meet the electricity demand and the deficit is covered by fossil electricity generation. However, already in the second week of February, the renewable energy production has caused a significant surplus of energy production. These surpluses can not be stored on the electricity grid and would therefore account as lost energy. Since these fluctuations would also occur due to the Dutch meteorological conditions, it is clear to see that with an increase in solar and wind energy, an increase in surpluses and deficits of energy can be expected. This would make the need for energy storage through the use of H_2 even more necessary than seasonal natural gas storage already is in today's world.

1.3. Subsurface storage in geological formations

Using the surpluses from renewable energy generation, water can be converted through electrolysis to produce the green energy carrier H_2. The produced green H_2 can then be stored in geological formations such as salt caverns, depleted gas and aquifers. This technique is also known as underground hydrogen storage (UHS) [12]. An overview of these geologic formations can be seen in Figure 1.3.1 [13].

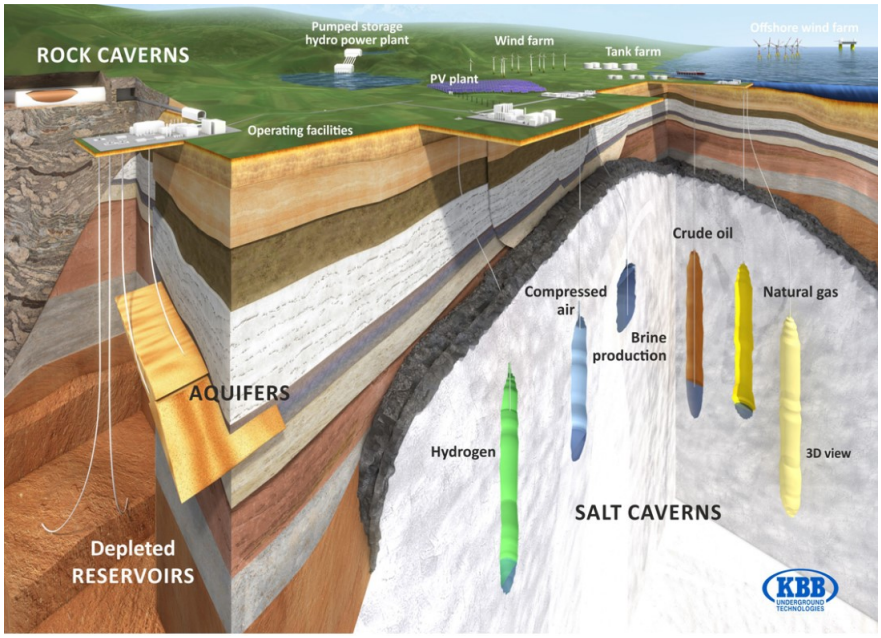

Figure 1.3.1: Visualization of potential geological storage sites for UHS [13]

In The Netherlands, storage of natural gas in depleted gas reservoirs has been executed since 1997 [14]. In Figure 1.3.2, an overview is given of the locations of all Dutch UGS sites are given. A total of four onshore gas reservoirs are currently used for seasonal storage of natural gas. These are the reservoirs of Norg, Grijpskerk, Bergermeer and Alkmaar. Since 2011, also salt caverns in Zuidwending are used for the storage of natural gas. In Winschoten, nitrogen gas (N_2) is stored in a salt cavern. This N_2 is blended in the natural gas infrastructure in The Netherlands to make the natural gas applicable for usage in the Dutch built environment [15].

On an international scale, UGS has rapidly increased over past decades. In total 680 UGS sites exists as of 2017 accounting for roughly 420 billion cubic meters (bcm) of stored natural gas [16]. UHS does not necessarily differ from UGS and therefore several similarly projects have already been conducted to investigate the appliance of UHS. For example, in Teesside, England and in Clemens, USA salt caverns are used to store 95% 'grey' H_2. This H_2 is then used as an industrial feedstock for chemical processes [17]. From 1956 to 1972 in Beynes, France, GDF stored a mixture of manufactured gas containing 50% 'grey' H_2 in a saline aquifer. The change in chemical composition of the gas in the reservoir proved the presence of microbial activity in the subsurface leading to the conversion of H_2 during UHS [18]. In both Argentina and Austria, a first feasibility study of UHS in a depleted gas reservoir site was performed. In Austria, a mixture of gas containing 10% H_2 combined with methane (CH_4) was injected into the

Figure 1.3.2: Locations of underground gas storage sites in The Netherlands [15]

reservoir. The results from the field test showed that 82% of the injected H_2 can safely be retrieved again from the reservoir [13].

1.4. Technical & economical Challenges of underground hydrogen storage

Just as with natural gas, H_2 can be stored in potential geological formations such as salt caverns, aquifers and depleted gas reservoirs. An overview of characteristics per type of geologic formation is given below.

Capacity

The storage capacity of above ground storage facilities in for example storage tanks is of a much smaller scale compared to the theoretical volumes found in the subsurface. The Netherlands largest above ground storage facility, the Gate Terminal has a volume of 0.3 bcm [19]. The storage capacity, of geologic formations is significantly greater. Especially for aquifers and depleted gas reservoirs, these potential volumes could easily range from 1-10 bcm [9]. This would provide energy storage capacity up to hundreds of GWh or several TWh in terms of natural gas or H_2. Salt caverns tend to have a smaller storage capacity and a single H_2 filled cavern is estimated to provide around 100 GWh of energy storage capacity [19].

Discharge Time

In order to use these storage sites efficiently high injection speeds for H_2 are essential in order to store as much H_2 as possible during periods of high H_2 production and low H_2 demand. Vice versa, H_2 production speeds need to meet the demand for H_2 during periods of energy shortage. Due to the relatively compact geometry and smaller volumes of salt caverns, changes in pressure can lead to high production speeds of H_2. For example, the N_2 filled salt cavern in Winschoten can produce up to 4,56 M m^3/day. In comparison with aquifers and depleted gas reservoirs, the maximum production rates per well are estimated at around 1 M m^3/day [9]. However, the usage of multiple wells at very high rates is strongly limited by the risk of induced seismicity.

Seismic Risks

When large pressure changes are applied to subsurface formations, risks of induced seismicity are always present. Salt caverns are man made structures that need to be constructed through a process called solution mining. This process already could possibly lead to local effects such as subsidence [9]. The use of depleted gas reservoirs is generally less prone to seismic risks. In the past, natural gas production from this reservoir has provided sufficient knowledge of the subsurface in this area. This knowledge can be used to quantify the possible risks related to

seismicity. Aquifers generally have not been depleted prior to the usage as a storage facility. Therefore, a lot of uncertainty is linked to the local behaviour of the subsurface when pressure differences are applied. Without extensive research of the effects of these pressure changes on the subsurface, increased risks of induced seismicity during cyclic storage will occur. However, oil and gas production are traditionally mainly characterized as depletion processes. The extraction of these natural resources leads to a constant pressure decline in the subsurface. In comparison, during cyclic storage, the pressure in the subsurface will always be maintained between a safe upper and lower limit reducing the risks of seismicity [9].

Cushion Gas
During the cyclic storage of gasses in geological formations, only a share of the total theoretical volume of the reservoir can be used. Prior to the cyclic storage of H_2 a large amount of gas needs to be injected in the subsurface in order to maintain a minimum pressure in the cavern or reservoir. Maintaining this minimum pressure in the subsurface will limit the risks for induced seismic activity. The gas that is used to guarantee this stability is called cushion gas and ideally remains permanently in the storage site. Salt caverns need less cushion gas due to their compact geometry and generally smaller scale. Depleted gas reservoir and aquifers on the other hand are often characterized by their wide and elongate structures. Since this cushion gas will not be used for the seasonal storage for energy, the main criteria for cushion gas is that it is cost efficient and that it will maintain the minimum pressure in the subsurface. In order to keep the concentration H_2 as pure as possible in the storage site, H_2 itself could be used as a cushion gas. However, due to the potential high production costs of H_2 this could be a costly option. Alternatively, N_2 is therefore proposed as a more cost-effective option. N_2 is also a less reactive gas and would therefore reduce the possibility of H_2 reacting with the cushion gas and other fluids [2]. Lastly, CH_4 could be used as cushion gas. However, more research is necessary regarding the reactivity between H_2 and CH_4 .

Costs
As mentioned before, salt caverns are man made structures that first need to be constructed before storage in the subsurface is possible. Since depleted gas reservoirs have already been used for the production of natural gas in the past, all knowledge of the subsurface and possible infrastructure is already present. This would not be the case for aquifers since generally no production has occurred from an aquifer in the past. The costs for the construction of a salt cavern including the necessary infrastructure for cyclic storage is estimated at around 334 €/MWh. The levelized cost of storage for cyclic storage of H_2 including the costs for infrastructure construction is estimated at 17 €/MWh per year [20]. In comparison, for depleted gas reservoirs the costs for constructing the new infrastructure are estimated between 280 - 424 €/MWh dependent on the size of the reservoir. The levelized costs of cyclic storage in depleted gas reservoirs are estimated between 51 to 76 €/MWh. Therefore, it is clear that reusing the existing natural gas infrastructure as much as possible could be a great financial benefit compared to salt caverns. For aquifers, the initial costs are not known. The operating costs for cyclic storage will be comparable to those of depleted gas reservoirs. No infrastructure is assumed to be present since there generally has not been production from an aquifer in the past meaning the total costs of establishing the storage facility will be significantly higher for aquifers.

Leakage
H_2 is the lightest molecule on Earth and can therefore easily leak away from subsurface storage facilities if no measures are taken. The wells and other materials that are normally used for oil and gas production are not necessarily applicable for subsurface H_2 storage and leakage through the materials could occur [18]. Also, the geologic formation itself could have pathways through which H_2 can migrate. For salt caverns this risk is relatively low since the H_2 will be surrounded completely by practically impermeable salt layers [17]. For depleted gas reservoirs, a proven seal or cap rock layer is present under which natural gas has been trapped over millions of years. For aquifers, a cap rock is present that proved to contain water in the reservoir rock. This does not mean that H_2 would also remain safely trapped under the same cap rock layer of depleted gas reservoirs and aquifers. Within the low permeable cap rock, a certain capillary threshold pressure exists which acts as the main sealing mechanism. Once this threshold pressure has exceeded, the rock could become permeable for gas and losses of H_2 would occur [21]. Moreover, (micro-) fractures in the cap-rock could provide migration pathways for H_2 to leak through.

Chemical Reactions
Aquifers and depleted gas reservoirs that contain sulphuric gas or minerals could potentially cause a reaction between H_2 and sulphur. This chemical reaction can create the highly toxic gas hydrogen-sulphide (H_2S). Also, this reaction will lead to acidification of the reservoir which could pose a threat to the integrity of steel alloys that are used at the storage site [18]. Chemical reactions between H_2 and the reservoir rock and fluids could lead to changes in porosity

and permeability impacting the storage space of a reservoir or aquifer. Decreases in porosity and permeability would lead to lower efficiency of storage cycles [22]. Furthermore, in all subsurface storage sites, microorganisms are present that can survive under subsurface conditions. These microorganisms potentially could convert H_2 to for example methane (CH_4) or again H_2S causing H_2 to be lost during storage cycles. This would lead to a decrease in storage efficiency.

	Capacity	Discharge rate	Initial costs	Cyclic costs	Seismic risks	Chemical conversion of H_2	Cushion gas need	Leakage risks
Salt caverns	Average	High	High	Low	Low	Low	Low	Low
Saline aquifer	High	Low	Average	Average	High	High	High	High
Depleted gas reservoir	High	Average	Average	Average	Average	High	High	High

Table 1.4.1: UHS Characteristics of different geological formations

An overview of all the factors that can positively or negatively impact the storage facility per geologic formation is given in Table 1.4.1. Summarizing the above mentioned technical and economical challenges, one can conclude that salt caverns are the most suitable for UHS. During a minimal need for safe storage of H_2, salt caverns provide the highest production speeds and account for minimal losses due to chemical reactions and leakage. Since also the safety risks are relatively low compared to other geologic formations, salt caverns are the most prudent choice for the initial development of UHS. Depleted gas reservoirs come next in terms of suitable geological formations for UHS. The large scale capacity of a single reservoir could potentially be the same as the storage capacity of several salt caverns. Also, the available knowledge of the subsurface and the possible reuse of existing infrastructure could be very useful when the reservoir needs to be transformed from production site to storage facility. Aquifers are initially the least suitable candidate for UHS. Most challenges are comparable to those encountered using a depleted gas reservoir. However, since there is generally no knowledge nor infrastructure present beforehand, depleted gas will be a more preferred alternative.

1.5. Problem Statement & Research Questions

The need for UHS in geological formations will depend on the scale of which H_2 will be used as CO_2 neutral energy carrier in the future Dutch energy landscape. The combination of fluctuating energy productions coming from renewable energy sources and a need for an alternative energy carrier other than electricity leads to a primary need for UHS. The huge volumes of geological formations such as depleted gas reservoirs, can potentially lead to the storage of hundreds of TWh in terms of energy capacity [19]. During the same time span in which renewable energy sources need to mature to become significant sources within the Dutch energy mix, the UHS technique needs extensive research before a subsurface H_2 storage site can be realized [19]. This research is needed mostly in the following fields:

- Usage of cushion gas and alternatives in presence with H_2
- Sealing degree of the cap-rock of the reservoir for different pressures and temperatures
- Geochemical reactions with H_2 and fluids and minerals within the reservoir system
- Biochemical conversion of H_2
- Mobility of H_2 and water to predict viscous fingering and sweep efficiency

In this research, all of the above mentioned topics will be investigated when applying UHS on depleted gas reservoirs. This will be done by conducting a literature study covering the listed topics and the current developments. Then, by performing a simulation study, the physical challenges of storing H_2 in porous media is addressed. By analyzing and reducing the energy loss, the efficiency of H_2 storage cycles in depleted gas reservoirs can be increased. Lastly, a sensitivity analysis will be performed to estimate the impact of different parameters on the potential of realizing an UHS site at a depleted gas reservoir. The link of UHS in geological formations and the above mentioned need for research in this field will be addressed using the following research question:

To what extent is hydrogen storage technically feasible in Dutch depleted gas reservoirs?

In order to better define the term feasibility the following sub-questions will be used to answer the research question:

- What is the necessary capacity for H_2 that needs to be met in order to define this storage technique as feasible?
- What losses of H_2 can be expected during the first and subsequent storage cycles?
- How can the hydrodynamic behavior between H_2 and residual fluids be described?
- What levels of cyclic efficiency can be achieved by utilizing a depleted gas reservoir as storage site?
- What is the impact of the simulation input parameters on the overall efficiency of this technique?

2

Potential of hydrogen energy storage in Dutch depleted gas reservoirs

Due to the large scale on which oil and gas production has been executed in The Netherlands a great amount of knowledge of the both the onshore and offshore subsurface is available. By comparing the gas-initially in place (GIIP) with the total production volume of a depleted gas reservoir, an estimation of potential storage capacity can be made.

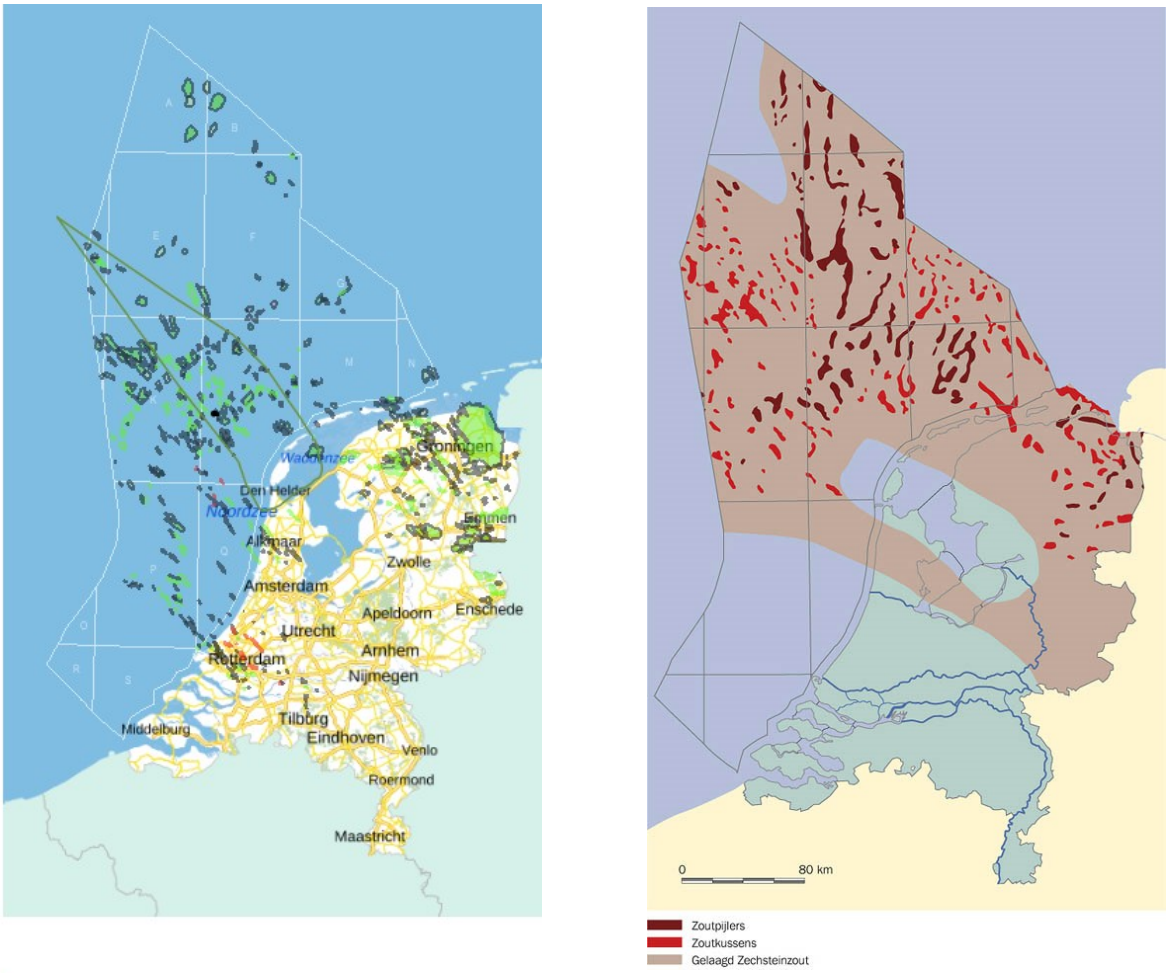

Figure 2.0.1: Overview of all oil (red) & gas (green) reservoirs in The Netherlands (left)
Presence of salt layers and domes in The Netherlands (right) [15]

From the aforementioned properties of the different potential geological formations, the conclusion was made that currently, in terms of efficiency and safety, salt caverns will be the most reliable geological formation to store H_2 into. Therefore, salt caverns will be used as much as possible for safe and reliable seasonal H_2 storage prior to depleted gas reservoirs.

In Figure 2.0.1, it is clear to see that the region where salt domes (red and dark-red planes) are present in the Dutch subsurface is limited to roughly the Dutch North-East onshore area and the North-West area offshore. Based on the onshore areas, it is assumed that a total of 321 salt caverns could be safely constructed here. The total effective storage capacity i.e. excluding the capacity occupied by cushion gas, is estimated at 14.5 bcm of H_2 [19]. Using the volumetric energy density for H_2 at standard pressure and temperature of 10.79 MJ/m^3, this volume can be converted to energy storage capacity [9] Therefore, the total effective volume in these salt caverns corresponds to an energy storage potential of **156 PJ** (43.3 TWh) [19]. Due to the current lack of worldwide knowledge and experience with the construction of salt caverns offshore, the potential storage capacity of offshore salt caverns is excluded.

In Figure 2.0.1, it is clear to see that the dimensions of the gas reservoir can vary a lot. Also in terms of location, there is a wide variety of where these gas reservoirs can be found in The Netherlands. The largest onshore gas reservoirs are found in the northern part of The Netherlands. The most dense concentration of multiple gas reservoirs can be found in a few areas offshore. The total amount of effective storage capacity in depleted gas reservoirs is estimated at 153 bcm of H_2 [9]. Therefore, the energy storage capacity through the use of H_2 in depleted gas reservoirs is estimated at a total of **1641 PJ** (456 TWh).

2.1. Quantitative need for H_2 storage

In several scientific studies regarding large scale green energy storage, different predictive models are used leading to scenarios that describe the use of different energy sources in the future energy mix. In order to quantify the future need for H_2 storage in The Netherlands, the results of the report: '*Klimaatneutrale Energiescenario's in 2050*' by Berenschot & Kalavasta is used. This report is developed in cooperation with different network operators in order to give an insight of the necessary energy infrastructure during the energy transition [23]. The final need for energy storage in The Netherlands in 2050 trough the use of H_2 is a combination of the usage of H_2 in the future energy landscape and the meteorological conditions occurring throughout the year. Berenschot & Kalavasta sketch the potential usage of H_2 in The Netherlands according to four strategic and policy related scenarios:

Regional Management	**National Management**
100% CO2-reduction in The Netherlands	100% CO2-reduction in The Netherlands
No import of energy	Minimal import of energy
Decrease of energy-intensive industry	No change in energy-intensive industry

European Management	**International Management**
100% CO2-reduction in The Netherlands	100% CO2-reduction in The Netherlands
European hydrogen market	Global hydrogen market
Growth of energy-intensive industry	Growth of energy-intensive industry

Table 2.1.1: Highlights key assumptions from the different management scenario in *Klimaatneutrale Energiescenario's in 2050*

In the above table, a few key assumptions of each management scenario are highlighted. The full definition for each scenario can be found in the Appendix. One can see that in the National Management scenario, the assumption is made that The Netherlands will rely on a fully sustainable and self-sufficient energy system. In this energy system, mismatches of energy supply and demand will be covered through energy storage of green gas and H_2. Since the Dutch energy system will be self-sufficient, this automatically means that there is no import nor export of H_2 or other energy carriers taking place. The primary need for H_2 storage will therefore arise from the need for seasonal energy storage. In comparison, in the European and International Management scenarios the main assumption is made that H_2 production and consumption will be governed through import and export with other countries. Due to the lack of storage space in other countries, The Netherlands will serve as an import country for the import and strategic storage of H_2. Therefore, the great share of the need for H_2 storage is caused by strategic H_2 storage.

Besides management related scenarios, Berenschot & Kalavasta also analyze the historically occurring meteorological conditions in The Netherlands. The meteorological conditions of 2015 in The Netherlands are defined

as an average year which is likely to return more often in the coming decades. The 2015 year is defined by mild fluctuations in temperature and the regular presence of ideal conditions for the generation of wind and solar energy. The weather during the year 1987 in The Netherlands is seen as an extreme year with a sharp decrease in average temperature throughout the year leading to an increased demand for heat and energy throughout the winter. Also, a great deficit of energy production from renewable energy sources will lead to an extra need for energy storage to cover for such harsh conditions. From the combination of the above scenarios, the minimum need for H_2 storage is found during the National Management scenario in combination with the mild 2015 meteorological conditions. This need for storage in 2050 corresponds with a total volume of 5.3 bcm of H_2 or in terms of energy **57.2 PJ** (15.9 TWh). Since the different potential geological formations have both positive and negative aspects when it comes to UHS, a suitable combination of geological storage sites need to be defined. This combination will be done using the priority scheme defined at the end of Chapter 1. As described before, due to the lower efficiency and higher leakage risks of H_2 storage in depleted gas reservoirs, the need for storage should initially be covered by salt caverns as much as possible.

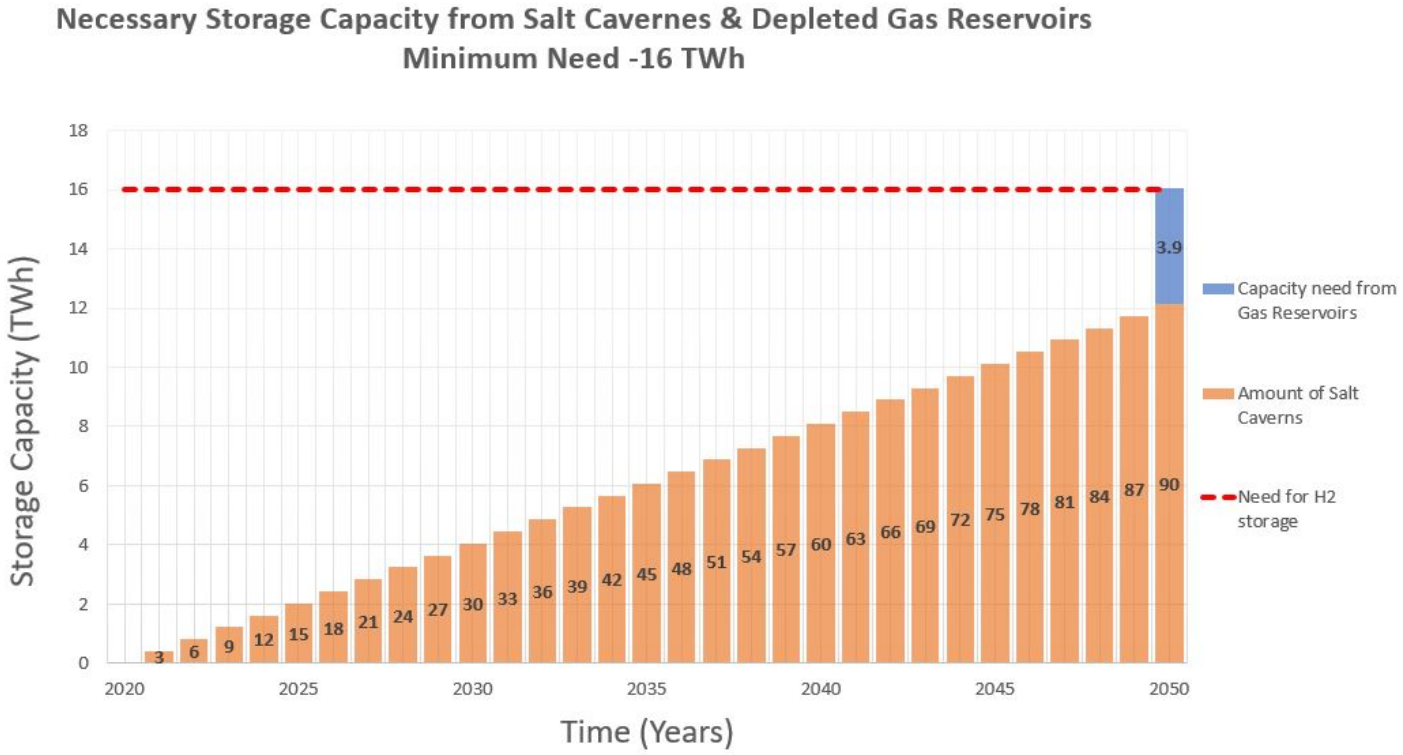

Figure 2.1.1: Minimal need for seasonal H_2 storage in Dutch depleted gas reservoirs

A limiting factor for constructing salt caverns is the construction capacity rate in The Netherlands. With the current capacity, a total of three salt caverns per year can be constructed [19]. Starting in 2020, the yearly construction of salt caverns at maximum construction rate could therefore realize 'only' 90 caverns in 2050. This would corresponding to an effective capacity of 12.1 TWh. Compared to the minimum need for H_2 storage in 2050, this would lead to a storage deficit of 3.9 TWh of H_2. Since depleted gas reservoirs currently serve as the best alternative to salt caverns, this deficit could best be covered by the usage of large depleted gas reservoirs with a total of 11.5 bcm of work volume.

2.2. Properties of gas reservoirs in The Netherlands

Understanding the geological setting of depleted gas reservoir in The Netherlands is essential to understand the heterogeneity in reservoir properties that is present across the subsurface. From figure 2.0.1, one can see that most greatest onshore and offshore gas fields can be found in the northern part of Netherlands.

The field data for several offshore reservoirs in the The Netherlands is made available by TNO. The reservoir properties that are provided include mean porosity, reservoir dimensions, GIIP, initial reservoir pressure. These are

essential input parameters that will be used for the eventual simulation of cyclic H_2 in a depleted gas reservoir. Since only the minimum, maximum and average permeability and porosity are known, the average values are used for the homogeneous reservoirs. An overview of these parameters can be found in the Appendix. According to TNO, the total of the 456 TWh of effective storage capacity is subdivided into two groups. There are 73 gas reservoirs onshore with together an effective work volume of 109 bcm. Another 67 suitable offshore gas reservoirs could provide 67 bcm of work volume capacity [19].

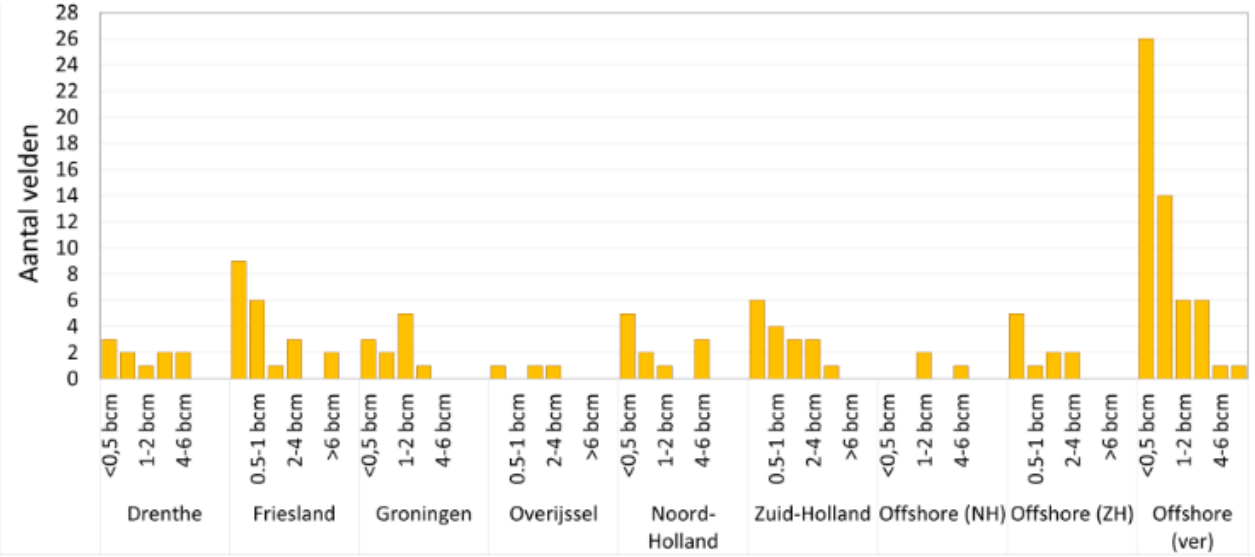

Figure 2.2.1: Overview of available work volume in gas reservoirs in different Dutch areas [9]

The great variation in reservoir capacity is best visualized in the histogram above showing the different sizes and locations of these reservoirs throughout different regions in The Netherlands. The great variety in capacity of suitable reservoirs in different regions provides the opportunity to use different storage strategies for area matching with the regional need and preferences when it comes to H_2 storage. As stated before, a total capacity of at least 11.5 bcm of work volume aside from salt caverns is necessary to meet the minimum demand for H_2 storage capacity in 2050. This roughly corresponds with twice the size of the existing onshore storage facility Norg in Groningen [9] From Figure 2.2.1, one can also see that this storage capacity is also available by using for example the two largest suitable gas reservoirs in the region 'Offshore Ver'.

3

Physical & Chemical Behaviour of Hydrogen in Porous Media

In this chapter an overview of the essential properties of compressed H_2 gas will be provided. Furthermore, the complex issues and challenges that occur due to the unique properties of H_2 gas when transporting compressed H_2 into a depleted gas reservoir, will be addressed independently.

3.1. Properties of hydrogen

Hydrogen (H) is the most abundant and lightest element that can be found in on Earth. H_2 gas is considered to be a non-toxic, odorless and colorless gas. The melting point can be found at 14 K whereas the boiling point is already found at 20K at atmospheric pressure [24]. These properties make it extremely difficult to store hydrogen under standard atmospheric pressure and temperature. Whereas other gases can be liquefied around the standard temperature of 293 K, this is unfortunately practically impossible for H_2. In Figure 3.1.1, three different combinations of pressure and temperature are given for different storage technologies [25].

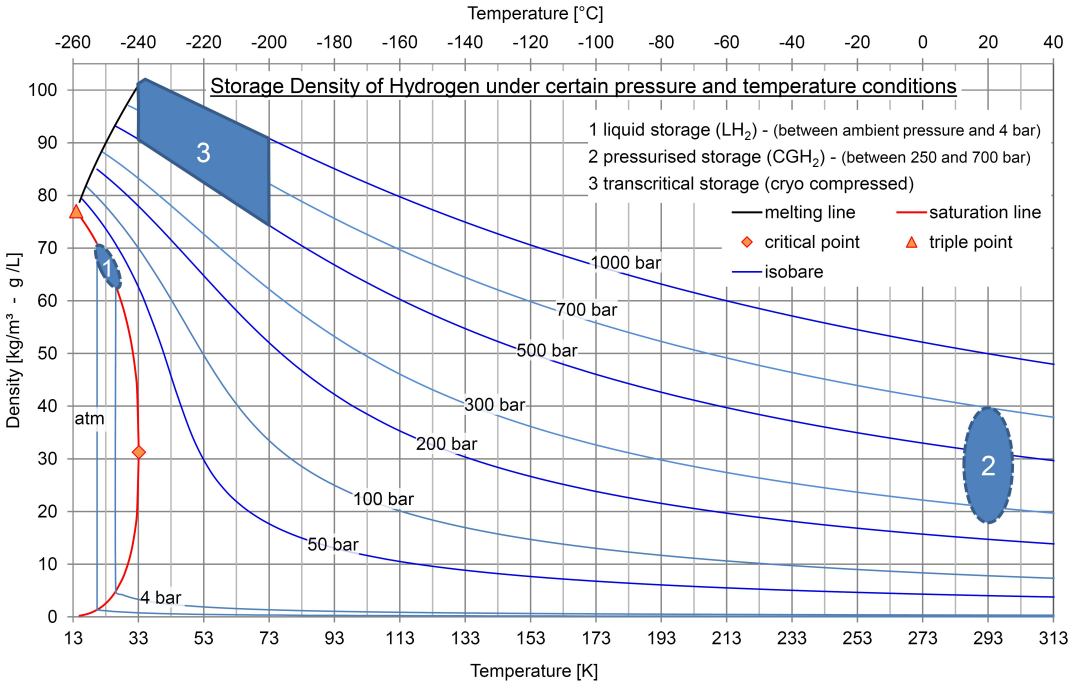

Figure 3.1.1: Storage Density of Hydrogen under certain pressures and temperature conditions. (1) liquid storage, (2) compressed gas storage, (3) cryo compressed storage [25]

Since liquid storage and cryo-compressed storage need extremely low temperatures for storage, only compressed storage can be applied to subsurface storage sites. For pressure ranges between 50 - 300 bar, and temperature between 300 - 400 K, H_2 can safely be stored as a gas. From Figure 1.1.1, it becomes clear that H_2 can only transport large amounts of energy when it can accumulate in a small volume, for example by pressurizing the gas. Leaks of H_2 in open spaces are not seen as a threat due to the very low density of H_2 making accumulation in the air improbable. In closed spaces, leakage could pose significant risks [5].

3.2. Reactivity of H_2 in reservoirs

H_2 is characterized as a highly reactive element. In subsurface reservoirs a certain chemical equilibrium exists prior to injection or production. Introducing H_2 to the reservoir causes a disturbance of this equilibrium which can lead to both geochemical and biochemical reactions. The reactivity of an element is based on the the reduction-oxidation (RedOx) potential at different pressures and temperature. This potential described the likelihood of a material to either accept electrons (reduction) or donate electrons (oxidation) [7]. The half reactions taking place for H_2 read

$$H_2 = 2H^+ + 2e^-. \tag{3.1}$$

The other way around, H^+ ions have the ability to accept electrons and therefore to generate H_2. The overall complete RedOx reaction is described as

$$O_x + \frac{n}{2}H_2 = R_{ed} + nH^+. \tag{3.2}$$

Here O_x is used as a term to describe a half reaction of an oxidant. Likewise, R_{ed} is used to describe the corresponding reducer of this half reaction. From Equation 3.2 is clear to see that H_2 is a electron donor. During the oxidation, 1 mol of H_2 has the ability to donate two electrons through RedOx reactions.

3.2.1. Geochemical Reactions

The injection of H_2 will lead to a disturbance in chemical equilibrium within the reservoir. This will induce geochemical reactions between H_2 and the reservoir which can lead to dissolution or precipitation of minerals present in the reservoir rock or fluid. This therefore could have an effect on properties such as the porosity and permeability of the reservoir rock potentially leading to changes in productivity and stability of the reservoir [7]. It is therefore essential that knowledge of the chemical composition of the reservoir rock and fluids are known prior to injection of H_2 to the storage site. This can be done by, for example, performing a field study at natural gas storage sites or laboratory experiments focusing on gas-fluid-interactions. Precipitation of minerals could also have a positive impact, for example on the caprock where a decrease in porosity or permeability contributes to a higher integrity of the caprock towards H_2. An increase in porosity due to dissolution could on the other hand lead to a higher loss of H_2 due to leakage. A PHREEQC study showed that at 40^oC and 40 atm the storage of H_2 induces the precipitation of minerals as K-feldspar, kaolinite and dolomite in the reservoir [22]. Dissolution of minerals as quartz, calcite and illite can occur simultaneously. These volume changes can lead to changes in porosity. This study calculated the absolute change in porosity as a net decrease of 0.05%-0.21% [22].

3.2.2. Biochemical Reactions

During UHS, H_2 consumption by microbial activity is most likely to occur leading to changes in the chemical equilibrium and conversion of H_2 . Bacteria consume the energy that is produced from the RedOx potential of H_2 [17]. Evidence of this activity can be found from town gas storage sites in Lobodice, Czech Republic and Beynes, France [18]. There are three main biochemical reactions likely to occur when storing H_2 in porous media:

- Methanogenesis:

$$CO_2 + 4H_2 \rightarrow CH_4 + 2H_2O \tag{3.3}$$

  Methanogenesis occurs when microorganisms are exposed to the presence of both H_2 and CO_2. CO_2 can be present in the reservoir as one of the minerals of the reservoir rock or by co-injection with H_2 into the reservoir.

- Acetogenesis:

$$2CO_2 + 4H2 \rightarrow CH_3COOH + 2H_2O \tag{3.4}$$

  Microorganisms causing acetogenesis will cause a pH-value decrease and are often found in UGS reservoirs. These organisms are capable to survive up to temperature of 90^oC and high levels of salinity.

- Sulfate-Reduction

$$SO_4^{2-} + 5H_2 \rightarrow H_2S + 4H_2O \tag{3.5}$$

  Sulfate-Reducing-Bacteria (SRB) can generate great volumes of the highly toxic hydrogen sulphide (H_2S) causing increased safety risks at the storage site. Also, this reaction leads to significant acidification of the reservoir which could pose a threat to the integrity of steel alloys using at the storage site.

In order to reduce the effects caused by this microbial activity the reservoirs used as storage facility should be high saline and have a reservoir temperature well above 90^oC . A numerical model based on PHREEQC showed that for depleted gas reservoirs two hotstpots in the reservoir for the conversion of H_2 to H_2S can be identified. These are the contact area of the H_2 with the caprock and the contact area of the H_2 with the underlying rock [22]. At both locations, the constant consumption of sulfate by SRB is balanced by a constant diffusion based supply additional sulfate. Moreover, at the contact area of the H_2 with the underlying rock also additional CO_2 is delivered using the same transport mechanism leading to an increased concentration of CH_4 here. By having a infinite supply and of CO_2 and sulfate, the losses due to microbial conversion in low saline gas reservoirs with a low temperature could be up to 50% in a timespan of 30 years [22].

3.3. Multi-Phase Flow in Porous Media

In order to store the H_2 safely in the subsurface reservoir, the H_2 needs to be pumped into the pores of the reservoir rock. Prior to the storage the pores of a depleted gas reservoir are filled with either unrecoverable residual natural gas or brine. Therefore, when injecting gaseous H_2 within the reservoir rock, the H_2 will displace the residual fluids inside the pores. This behaviour of the gaseous H_2 within the pores of the reservoir rock can be predicted by applying both (i) Darcy's law and (ii) the law of mass conservation for two-phase flow.

(i) Darcy's law for two-phase flow describes how this fluid is transported through a porous medium. The velocity at which the fluids passes through the reservoir is calculated using the following relation [2]:

$$q_\alpha = -\frac{k k_\alpha^r}{\mu_\alpha}(\nabla P - \rho_\alpha g \nabla z) \ , \ \alpha = l, g \tag{3.6}$$

Here, k is the absolute permeability, k_α^r is the relative permeability of phase α, μ_α is the viscosity of phase α, ∇P is the pressure gradient applied on the reservoir, ρ_α is the density of phase α and g is the gravitational acceleration acting on ∇z direction. Moreover, q_α is the Darcy velocity of the fluid phase α.

(ii) For flow of both the phases in porous media, the conservation of mass is applied. This law is described as follows [2]:

$$\frac{\partial}{\partial t}(\phi \rho_\alpha S_\alpha) + \nabla \cdot (\rho_\alpha q_\alpha) - q_\alpha^0 = 0, \quad \alpha = l, g \tag{3.7}$$

Where ϕ is the porosity of the reservoir rock, S_α is the saturation factor of phase α and $\boldsymbol{q}$ is the Darcy velocity of the transported fluid.

Moreover, it is assumed that the phases fill up the entire pore space, i.e.,

$$\sum_\alpha S_\alpha = 1. \tag{3.8}$$

3.4. Compressibility

During flow of fluids in porous media changes in pressure causes different forces to be exerted on the reservoir rock and fluids. These forces lead to changes in the volume of both the fluids present and on the pore space inside the reservoir. This phenomena is called fluid and rock compressibility. Fluid and rock compressibility have a great effect on the effective storage capacity of a reservoir. For example, in extremely low permeable zones inside a reservoir, the effective capacity that can be used for storage is limited to the compressibility of the rock and the fluids. In this way compressibility of fluids will lead to a significant pressure increase and could cause geo-mechanical damage to the caprock and the reservoir rock [26].

Mass balance equations described before include the fluid compressibility via the density term. This can be further extended by introducing the fluid compressibility as $c_\alpha = (\frac{1}{\rho_\alpha})(\frac{d\rho_\alpha}{dP_\alpha})$ [27]. The compressibility of gasses at reservoir conditions is significantly higher than that of e.g. liquids and rock [27, 28].

Typical Range of c_α values	c_α $[Pa^{-1}]$
Rock	$10^{-11} - 5 \cdot 10^{-9}$
Water	$4.5 \cdot 10^{-10}$
Gas	$1 \cdot 10^{-7} - 1 \cdot 10^{-9}$

Table 3.4.1: Typical Range of Compressibility Values [27]

Gasses are one to two orders of magnitude greater in terms of compressibility compared to rock and water for example. During this study rock compressibility will be neglected since the used pressures for storage are not high enough to cause any significant changes to reservoir rock [27].

3.5. Complexities with Hydrogen Storage in Porous Media

The properties of H_2 differ a lot from the properties of conventional storage gasses such as natural gas. Both the density and viscosity of H_2 are significantly lower compared to natural gas influencing the behaviour within porous media. Also, compared to natural gas, H_2 has a lower heating value meaning that more storage capacity is necessary in order to store the same energy capacity per mass unit [1].

3.5.1. Solubility

During UHS in porous media, H_2 will get into contact with brine in the reservoir. This will lead to dissolution of the gas into the brine. The dissolution of hydrogen needs to be understood since it leads to increments in pH values and reduces the RedOx potential [29]. Also the dissolution of gas into liquid could lead to losses of H_2 during storage. The solubility of a gas in a liquid can best be described by Henry's Law:

$$c_{g,w} = \frac{P}{K_H} \tag{3.9}$$

Here $c_{g,w}$ equals the concentration of the gas in the liquid phase, K_H denotes Henry's constant and P is the partial gas of the specific gas under equilibrium conditions [7]. K_H is species, temperature and pressure dependent [30].

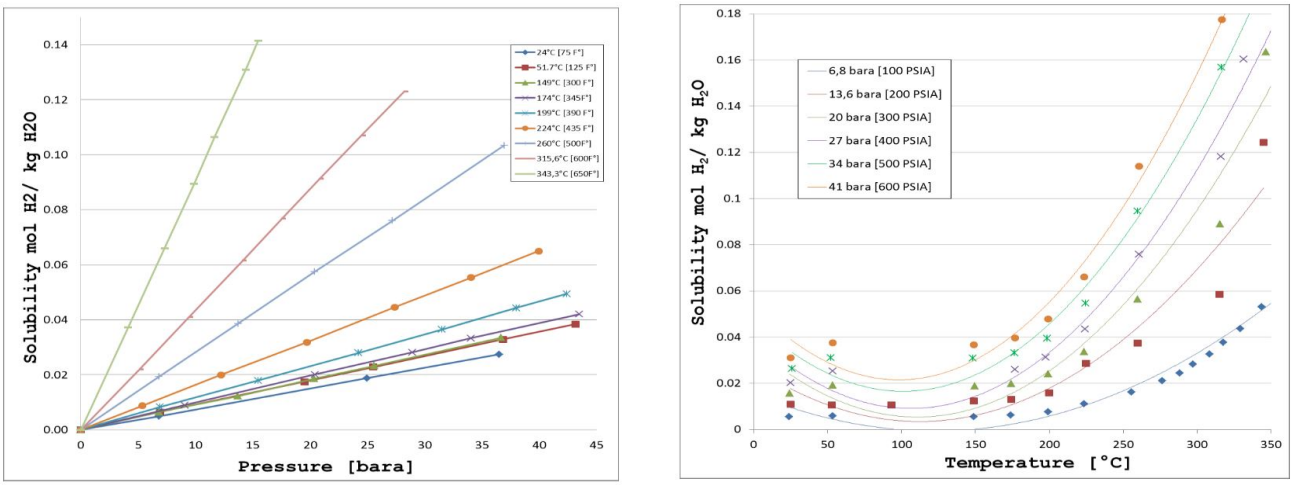

Figure 3.5.1: Solutbility of H_2 in water at different pressure and temperature [29, 31]

For H_2 under different pressure and temperature, the solubility is visualized in Figure 3.5.1 [29, 31]. One can see that the solubility of H_2 in water decreases until 100 ^oC . At higher pressures the solubility starts to increase again. The solubility increases linearly with pressure as can be observed from Figure 3.5.1. Since the phenomena of dissolution is based on changes in equilibrium, the losses due to dissolution of the H_2 can be seen as a capital loss instead of an operational loss. After injection of H_2 the disturbance in equilibrium will be balanced again and additional dissolution will be unlikely to occur. The total once only loss due to the dissolution of H_2 in brine are expected to be 2% of the storage capacity [32]. From a successful field study test in Austria using 10% H_2 in the injected gas, the loss due to dissolution where estimated at 0.88% [13]

3.5.2. Viscous Fingering

During displacement of fluids in porous media, mobility differences between the injected and displaced phase can lead to so called viscous fingering. During gas-water displacements the highly mobile gas will try to find pathways through the relatively viscous water.

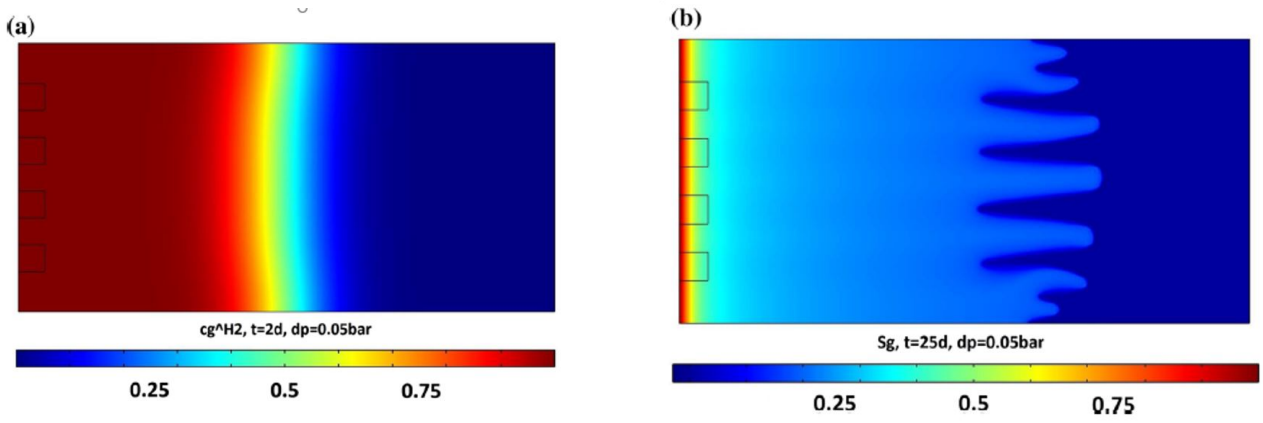

Figure 3.5.2: Stable gas-gas displacement (a) and viscous fingering during gas-liquid displacement (b) [17]

This effect is shown in Figure 3.5.2 [17]. The occurrence of viscous fingering can be described by the mobility ratio between the respective fluids according to the following formula:

$$M = \frac{k_{rg}/\mu_g}{k_{rw}/\mu_w} \tag{3.10}$$

If M<1, the displacement process is considered to be stable and efficient whereas an M>1 implies unstable displacement and thus the occurrence of viscous fingering. In depleted gas reservoirs displacement between a cushion gas or residual methane is considered. H_2 displacing another gas is considered to be 10 times faster than the unstable displacement of water by H_2 [33].

3.5.3. Gravity Override

The effect of gravity is of great importance during UHS. Due to density differences among fluids the lighter fluids will easily rise and accumulate above fluids with a high density. This phenomena is described as gravity override and reduces the overall efficiency of displacement processes in porous media. Since H_2 is a very low dense gas, this buoyancy effect will be noticeable when displacing almost any gas or liquid [34].

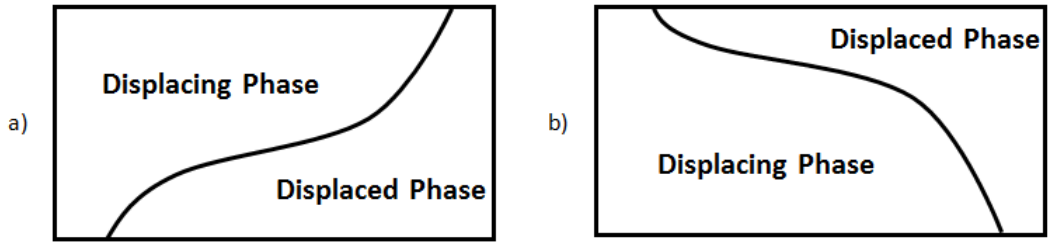

Figure 3.5.3: Gravity segregation in displacement processes. a) Gravity override b) Gravity underride [34]

On the other hand, gravity override can also be of beneficial use during UHS operation. Injection of cushion gas by for example N_2 could displace a more dense residual gas or liquid. Due to gravity override the N_2 will then rise above the heavier residual fluid. Consequently, when afterwards H_2 is injected in this subsurface, H_2 will be in contact with cushion gas N_2 instead of the residual gas or liquid [7].

In this report the used fluids will always be pure H_2 gas in contact with other mixtures or pure gasses. Therefore, the different gas components will differ in properties such as density, viscosity and compressibility. Since H_2 is the lightest gas molecule that can be found in our atmosphere, the phenomena of gravity override is most likely to occur in the presence of other fluids within the porous media. The ratio of viscous and buoyancy forces during the transport

of gasses in porous media is quantified using a dimensionless gravity number N [35]. For compressible fluids the gravity number is as follows:

$$N = \frac{k\Delta\rho g\rho_c 2\pi r_c d}{\mu_{H_2} Q_m} \tag{3.11}$$

Here, k is the intrinsic permeability of the reservoir, $\Delta\rho$ is the difference between the fluids, r_c is the radial length, d is the reservoir thickness μ_c and Q_m is the mass flow rate of H_2 [27]. The mass flow rate is chosen since accounting for the compressibility in this system will lead to variable volumes and therefore densities. ρ_c is the characteristic density and can be chosen as the mean of the injected H_2 plume. For the sake of simplicity the decision is made to assume a linear relationship between the gas components and the pressure. This is described by the following formula:

$$\rho_c = \rho_0 + \rho_1\beta(P_{H_2} - P_{t_0}) \tag{3.12}$$

where ρ_0 and ρ_1 are respectively the initial and present density of H_2. β is the compressibility factor of H_2. P_{H_2} and P_{t_0} are the reference pressure for ρ_0 and ρ_1 . For large gravity number $(N >> 1)$, gravitational forces are dominant during the transport of the gas. For smaller gravity numbers $(N << 1)$ viscous forces are seen as the dominant transport mechanism [27].

However, the analytical solution proposed by does only focus on the density difference between a compressible injected fluid relative to an incompressible displaced phase. Moreover, the viscosity of the displaced phase is not taken into account.

Therefore, another analytical solution described is additionally is used as well. Another dimensionless parameter $\gamma_{g_{inj},g_{res}}$ describes the the relative importance of viscous and gravitational forces [36]. This solution does not take compressibility of both phases into account. However, the difference in both density an viscosity are necessary making it possible to analyze the ration in effective gravitational and buoyancy forces. This dimensionless parameter is obtained as follows:

$$\gamma_{g_{inj},g_{res}} = \frac{Q_o}{2\pi k d^2 g}\frac{\Delta\mu}{\Delta\rho} \tag{3.13}$$

Here, $\Delta\rho$ is the difference in density between the injected and residual gas, d is the reservoir thickness, $\Delta\mu$ is the difference in viscosity of the respective fluids and Q_o is the volumetric flow rate of the injected fluid. This is calculated using $Q_o = \frac{Q_m}{\rho}$.

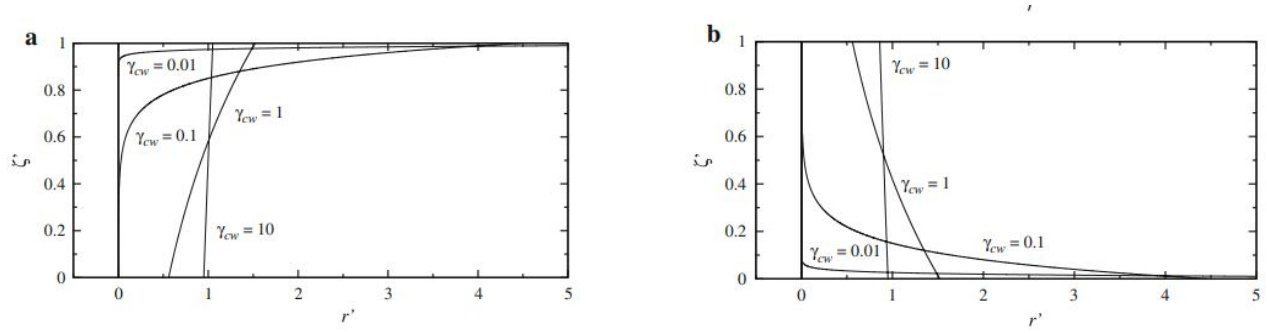

Figure 3.5.4: Predicted interface using γ for a less dense fluid injected into a more dense liquid (a) and for a more dense fluid injected into a less dense one (b) [36]

Dominant Forces	γ	N
Viscous	10^{-2}	10^{-3}
Comparable	10^{-1}	10^{-1}
Gravitational	10^{1}	10^{1}

Table 3.5.1: Definitions of dominant forces using N and γ [27,36]

For $\gamma_{g_{inj},g_{res}} > 0$, a less dense fluid displaces a more dense fluid. For $\gamma_{g_{inj},g_{res}} < 0$, this is vice versa. Comparable with the definition of the value of N, for values $0 > \gamma_{g_{inj},g_{res}} > 1$ gravitational forces are dominant during the displacement process. For $\gamma_{g_{inj},g_{res}} >>> 1$, viscous forces are the dominant component during displacement of the fluids.

3.5.4. Diffusion

The dispersion of H_2 in porous rocks needs to be also included in a feasibility study. Mass transfer due to dispersion consists of two components: molecular diffusion (D_d) and mechanical dispersion (D_m). Molecular diffusion occurs due to the random–so called Brownian–motion of the molecules caused by thermal kinetic energy. This movements are known to be isotropic and occur at all times, even in the absence of Darcy's velocity field. Mechanical Dispersion is split up in both longitudinal dispersion (parallel to the flow direction) and transverse dispersion (normal to the flow direction). Longitudinal dispersion has two main causes:
i) The flow velocity profile through pores changes from low velocity at the edges to high velocity at the center of the pores. ii) In a porous network the invading fluid will flow faster in greater pores than in smaller pores [37]. Transverse dispersion is caused due to the tortuosity of porous networks. Flow will follow the pathway branches within the porous networks and therefore the direction will differ from the original flow direction.

Mass transport of H_2 in subsurface porous media can be described by the sum of advection (J_a) and dispersion (J_d) fluxes. The advective flux reads

$$J_a = C\vec{u}. \tag{3.14}$$

Here, C is the concentration of the mass/unit of volume of the solution and $\vec{u}$ is the Darcy velocity. Dispersive flux can be also stated according to Fick's law as

$$J_d = -\phi\overline{D}\nabla C. \tag{3.15}$$

Here $\overline{D}$ is the sum of molecular diffusion D_d and mechanical dispersion D_m. The total flux $J = J_a + J_d$ needs to be included in the balance equation [33]. For example, for phase α, one can state

$$\frac{\partial}{\partial t}(\phi\rho_\alpha S_\alpha) + \nabla\cdot(\rho_\alpha J_\alpha) = \rho_\alpha q_\alpha, \tag{3.16}$$

where $J_\alpha = J_{a\alpha} + J_{d\alpha}$.

According to [38], the diffusion coefficient is calculated by

$$D_{\text{diff},g} = \phi S_g \tau\Big(\sum_{j=1\neq i}^{n} \frac{c_g^j}{\tilde{D}_{\text{diff},g}^{i,j}}\Big)^{-1} \quad \& \quad D_{\text{diff},w} = \phi S_w \tau \tilde{D}_{\text{diff},w}^{k}. \tag{3.17}$$

The mechanical dispersion [38], on the other hand, is given by

$$D_{\text{disp},i}^{k} = \phi S_i\Big(\frac{v_i v_i^T}{||v_i||}(a_L - a_T) + ||v_i|| a_T\Big). \tag{3.18}$$

Here the term *a* represents the dispersivity in either longitudinal (L) or transverse (T) direction, and v is the flow velocity in the principle direction.

Since H_2 is a very small and light molecule, it can easily penetrate through any hole or fracture present in the reservoir. The low ability of H_2 to dissolute under reservoir conditions makes a water saturated cap rock a likely impermeable barrier for H_2 to migrate through. Losses of H_2 by diffusion through the cap rock are estimated to be between 2%-6% [13, 32]. The molecular diffusion coefficient for H_2 in water is considered to be $1 \cdot 10^{-}6\ m^2/s$ at standard conditions [33]. The coefficient for mechanical dispersion for H_2 is considered to be $5 \cdot 10^{-}4\ m^2/s$ [33].

4

Simulation Methodology

4.1. Introduction to Reservoir Simulation

In order to visualize the behaviour of H_2 displacing residual fluids and gasses in subsurface conditions, reservoir simulation is used as a tool to quantify the dynamics and sensitivities of the process. In the area of reservoir engineering, research is often conducted using laboratory experiments. Unfortunately, these experiments are always limited due to great difference in scale between the experiments and an actual reservoir. Geological data or results from laboratory experiments can be utilized as input parameters that will be utilized by the reservoir simulator. In this way the behaviour of a reservoir can be examined on a field scale. Common reservoir simulators discretize and solve partial differential equations that describe flow, transport and energy [39]. A suitable reservoir simulator for this research should incorporate the differences in density and mobility ratios between different gaseous components so that the characteristic hydrodynamic behaviour can be described.

4.2. Numerical Simulation in DARSim2

The Delft Advanced Reservoir Simulation research group of the faculty of Civil Engineering of the Delft University of Technology is established for the development of advanced modelling and simulation methods for complex processes in the subsurface geological formations [40]. The reservoir simulator used in this thesis is the MATLAB and C++ based dynamic reservoir simulator, DARSim2. This open-source simulator tool is developed to perform fully implicit method (FIM) simulations of multi-phase flow in both homogeneous and heterogeneous reservoir condition [40]. In order to simulate multi-phase flow within the reservoir the two fundamental conservation equations are used as described in Chapter 3. These are Darcy's law for flow in porous media (Eq: 3.6) and the conservation of mass (Eq: 3.7). According to these total bass mass balance equations, this means that in an open system the change in mass is always balanced.

4.3. Scenario Definitions

The reservoir simulator will be used for both 2D and 3D simulations. The 2D simulations will be used to describe the hydrodynamic behaviour of the H_2 in contact with the residual gas. The 3D simulations will be used to perform cyclic simulations. In this way, the performance of the reservoir for seasonal storage of H_2 can be analysed.

4.3.1. Fluid Parameters

In order to examine the hydrodynamic behaviour of H_2 in contact with different types of cushion gas, the choice is made to analyse the scenarios where:

- H_2 displaces N_2
- H_2 displaces an ideal gaseous mixture 80% N_2 & 20% CH_4

H_2 - N_2 - Displacement

The H_2 - N_2 case simulates the process in which H_2 displaces the cushion gas N_2. The following fluid parameters have been assigned for the respective components in the reservoir [28, 41].

	Parameter	Value
ρ_{S_1}	6.18	kg/m^3
ρ_{S_2}	87.4	kg/m^3
μ_{S_1}	$1.183 \cdot 10^{-5}$	Pa· S
μ_{S_2}	$2.09 \cdot 10^{-5}$	Pa· S
$c_{g_{S_1}}$	$8.3 \cdot 10^{-8}$	Pa^{-1}
$c_{g_{S_2}}$	$1.43 \cdot 10^{-8}$	Pa^{-1}

Table 4.3.1: Fluid properties of S_1 = hydrogen gas and S_2 = nitrogen gas [28,41]

Note that the initial density values here given at $P = 100$ bar. Due to compressibility of both gas components, these values will change over time. Here, S_1 is the injected component and thus H_2 whereas the residual phase N_2 is denoted by S_2 . The simulation assumes an injection of 100% H_2 whereas the gas initially present in the reservoir consists of 100% N_2. The compressibility factor c_g for each gas component is obtained by linearly interpolating the values for the gas density given at at respectively the minimum and maximum pressure that is set for each simulation.

H_2 - N_2 - CH_4 Displacement

The H_2 - N_2 - CH_4 case simulates the process in which H_2 displaces an ideal mixture that is used as cushion gas. This mixture consists of 80% N_2 and 20% CH_4 The following fluid parameters have been assigned for the respective components in the reservoir.

	Parameter	Value
ρ_{S_1}	6.86	kg/m^3
ρ_{S_2}	80.8	kg/m^3
μ_{S_1}	$1.03 \cdot 10^{-5}$	Pa· S
μ_{S_2}	$1.94 \cdot 10^{-5}$	Pa· S
$c_{g_{S_1}}$	$8.3 \cdot 10^{-8}$	Pa^{-1}
$c_{g_{S_2}}$	$1.45 \cdot 10^{-7}$	Pa^{-1}

Table 4.3.2: Fluid properties of S_1 = hydrogen gas and S_2 = 80% nitrogen - 20% methane [28,41]

4.3.2. Reservoir Properties

This study will make use of both a homogeneous and heterogeneous reservoir. For both the homogeneous and heterogeneous cases, the reservoir has no angle of inclination. This means that the reservoir will have a completely horizontal orientation. Both the homogeneous and heterogeneous reservoir will be composed of mesh grid consisting of equidistant grid cells with no changes in grid cell size throughout the reservoir cells. The boundaries of the reservoir are so called Dirichlet boundary conditions, meaning no flux is possible to pass through. At the location of the well a constant (in)flux is considered which are Neumann boundary conditions.

Homogeneous Reservoir

For the homogeneous 2D and 3D test cases, geological input parameters are used based on the data of several depleted offshore reservoirs in The Netherlands. The chosen reservoir properties are a combination of several reservoir properties from depleted gas reservoirs with reservoir rocks of the Main Bundsandstein stratigraphical unit. This data was provided by NLOG [15]. An overview of the data from the Main Bundsandstein reservoirs is given in the Appendix. The dimensions of the reservoir and the change in injection and production pressure are based on the average values used in several numerical simulation studies regarding this topic [33] [42] [38].

Parameter	Value	Unit
Dimensions $L_x * W_y * H_z$	750 x 1 X 90	[m]
Grid Cell Size $d_x * d_y * d_z$	12.5 x 1 X 2.14	[m]
Injector Location (X,Y)	(1,1)	[m]
Producer Location (X,Y)	(750,1)	[m]
Well Perforation Zone (Z)	90	[m]
Injection Pressure	100	[bar]
Production Pressure	50	[bar]
Initial Reservoir Pressure	50	[bar]
K_{xy}	283	[mD]
K_z	32	[mD]
Porosity	0.127	[-]
Inclination θ	0	[^{o}]
Temperature	373	[K]

Table 4.3.3: Reservoir properties of the used homogeneous 2D reservoir

Heterogeneous Reservoir

In order to obtain results from the simulation that better reflect the real situation, heterogeneity of the reservoir is a vital aspect to include. Modelling a realistic reservoir can unfortunately not be based on the assumption that all reservoir properties are homogeneous in every direction. Introducing varieties in the porosity and permeability will have a significant impact on the hydrodynamic behaviour of H_2 in contact with different gasses. For the heterogeneous 2D and 3D test cases, a geostatistical model including the porosity and permeability of the Delft Sandstone aquifer was used. This aquifer will potentially be used for the realization of a geothermal energy doublet. Since the hydraulic properties of aquifers are generally more favorable than those of gas reservoirs, the porosity and permeability values that are assigned the box reservoir can be interpreted as highly favourable in comparison with the general reservoir properties for Dutch depleted gas reservoirs.The heterogeneity is introduced by giving the grid cells of the mesh grid of the reservoir different values for both porosity and permeability. A detailed visualization of the permeability and porosity throughout this reservoir can be seen in the Appendix.

Delft Sandstone Reservoir	Mean (μ)	Standard Deviation (σ)
K_{xy}	359 mD	88 mD
K_z	35 mD	8 mD
ϕ	0.158	0.098

Table 4.3.4: Average properties of the Delft Sandstone Reservoir

A few key reservoir properties have been listed in Table 4.3.4. Note that since this dataset if from an geothermal aquifer the porosity and permeability values in this case are on average more favourable compared to the homogeneous case. Compared to other Dutch gas reservoirs, such properties would be interpreted as highly favourable for a natural gas reservoir.

The dimensions assigned to the reservoir are for length and height respectively 750m x 90m. The combination of the porosity and permeability values throughout the reservoir also lead to the occurrence of so called high and low permeability streaks. In the homogeneous case, each grid cell was classified with a relatively high permeability and porosity. This would mean imply that the net-to-gross (N/G) of the reservoir is equal to 1. Using a heterogeneous reservoir, this ratio will sharply decrease. Therefore, when H_2 is injected in such a heterogeneous reservoir, preferential pathways are likely occur due to the presence of these permeability streaks. A 2D slice of the 3D data set is used to first hand describe the effects of introducing heterogeneity to the displacement of H_2 towards other gasses.

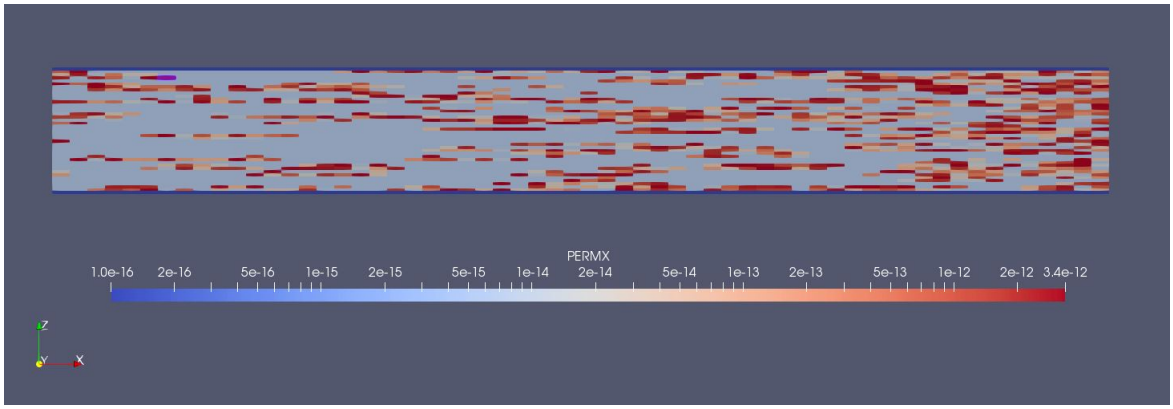

Figure 4.3.1: Permeability distribution of the Delft Sandstone model

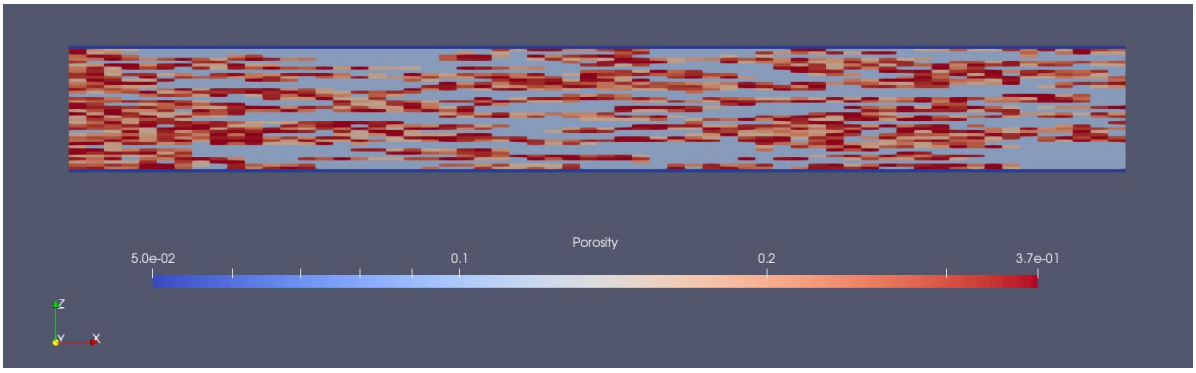

Figure 4.3.2: Porosity distribution of the Delft Sandstone model

In the above figures, the distribution in of permeability and porosity is visualized throughout the reservoir slice. It can be expected that the injected H_2 will penetrate more easily through the red zones shown in the above figures. The injecting well is placed on the far left side of the reservoir and perforated throughout the whole of the reservoir. The far right side of the reservoir is fully perforated by a producing well. The reservoir specific properties will logically change using the heterogeneous reservoir data set.

Parameter	**Value**	**Unit**
Dimensions $L_x * W_y * H_z$	750 x 1 X 90	[m]
Grid Cell Size $d_x * d_y * d_z$	12.5 x 1 X 2.14	[m]
Injector Location (X,Y)	(1,1)	[m]
Producer Location (X,Y)	(750,1)	[m]
Well Perforation Zone (Z)	90	[m]
Injection Pressure	100	[bar]
Production Pressure	50	[bar]
Initial Reservoir Pressure	50	[bar]
Average K_{xy}	1-1000	[mD]
Average K_z	0.1-100	[mD]
Porosity	0.1 - 0.35	[-]
Inclination θ	0	[^{o}]
Temperature	373	[K]

Table 4.3.5: Reservoir properties of the heterogeneous 2D reservoir

4.3.3. Main Assumptions

The scenarios that are studied using the reservoir simulator assumes only the presence of different gasses. The ability of the injected H_2 to displace another fluid or gas is in gas-liquid and liquid-liquid systems among others determined by the permeability of the reservoir rock towards each fluid. Since in this study only gas is present in the reservoir, it is assumed that there is no difference in permeability per gas component. Therefore, relative permeability is ignored. In order to carefully examine the effect of the viscous and gravitational forces, the two gas components are considered to be immiscible meaning that no mixing or diffusion processes are taken in to account.

Furthermore, since no equations of state (EoS) for H_2 are incorporated the DARSim2 simulator, the effect of temperature on the fluid properties will be neglected. Viscosity values for the used gasses will be based on a constant reservoir temperature which is chosen to be $373K$. This value is seen as the minimum temperature to limit the activity of the potential biochemical reactions described in Chapter 3 [18]. Other potential (geo-)chemical reactions are not taken into account during the displacement simulation. By excluding EoS, assuming incompressibility of the reservoir rock and assigning an isothermal temperature, changes in density of the gaseous components will be purely caused due to the compressibility of the gasses. Change in the respective fluid properties will therefore be limited to the density of the components caused by pressure gradients.

The 2D simulations will be used to analyze the ratio of viscous and gravitational forces, by investigating both N and γ during for both displacement cases in a homogeneous reservoir. The values for the gravity will provide the opportunity to quantify the behaviour of H_2. throughout the simulation.

The 3D simulation will be used to investigate the efficiency that can be achieved per cycle during seasonal storage of H_2. This will also be done using the same assumptions as described previously. The effect of including heterogeneity and the sensitivity of certain assigned input parameters in a homogeneous reservoir will be examined as well. Lastly, by incorporating the potential losses described by the various causes in Chapter 3, an overall efficiency of the seasonal storage can be given.

4.3.4. Gravity Number Analysis

Using the previously mentioned gravity number, an estimation can be made in order to quantify the displacement process to be either dominated by viscous forces or gravitational forces. For this analysis two different dimensionless gravity numbers are used. Due to the dependency of the characteristic distance (r_c) from the injections well, the gravity number N is used to analyze the ratio between the gravitational and viscous forces at different positions along the interface between the injected and residual gas. The calculation of N is done by using Equation 3.11. Using Equation 3.12 the effect of compressibility is taken into account in the calculation. The gravity number γ describes the average reaction between the gravitational and viscous forces regardless of the compressibility of the gas nor the position of the interface. This is done using Equation 3.13.

Parameter	Value	Unit
K	283	[mD]
$\beta = c_{S_1}$	$8.3 \cdot 10^{-8}$	[-]
d	90	[m]
g	9.81	$[m/s^2]$
Q_m	0.039	[kg/s]
Q_0	Q_m/ρ	$[m^3/s]$

Table 4.3.6: Parameters necessary to calculate the gravity number N [41]

The necessary parameters to calculate both gravity numbers are given in Table 4.3.6. The mass flow rate (Q_m) is based on the density of H_2 at standard conditions [28]. The volumetric flow rate (Q_o) is calculated using the actual density of the H_2 gas during the flow through the reservoir.

4.3.5. Cyclic Storage

By making additions to the DARSim2 reservoir simulator, cyclic storage simulations are implemented in such a way that the overall simulation can be divided up into different stages. Hence, the reservoir state during the last time step of stage x will be the initial state of the reservoir for stage $x+1$. Using this methodology the injection and production phases described in the beginning of this chapter can be performed independently

In order to demonstrate the pressure behaviour exerted on a gas reservoir during seasonal energy storage, different stages are assigned during the cyclic simulations. There are four main stages that normally would take place during the storage of H_2 in gas reservoirs:

1. Depletion of the reservoir until the desired state reservoir state is reached
2. Injection of the cushion gas in the depleted gas reservoir
3. Injection of H_2 in the remaining work volume of the reservoir
4. Cyclic production and re-injection of H_2 in the reservoir.

During the cyclic simulations, the initial state of the reservoir swill be set to the pressure that can be found in a depleted gas reservoir that is already filled with cushion gas. Therefore, the first stage will not be shown in the cyclic simulation results. Since the simulation assume that the residual phase it cushion gas, the second stage is also not used as a separate simulation stage. In both the 2D and 3D results two full injection and production cycles are simulated.

The dimensions assigned to the reservoir are set as follows for length, width and height respectively 750m x 750m x 90m. The reservoir data set has a mesh grid of 60 by 40 by 42 (X,Y,Z) corresponding to cell dimensions of 12.5 m by 12.5 m by 2.14 m. The position of the injector well is at the center of the reservoir i.e. X,Y = 375m,375m. The injector well is changed to a producer after each stage and therefore the locations of both wells is kept the same. Perforation of the wells is throughout the whole depth of the reservoir which equals 90 meters. For the base cyclic storage scenario, the following reservoir states have been assigned for each stage:

Stage 1 (Injection)	Value	Unit
P_{inj}	100	Bar
P_{prod}	-	Bar

Stage 2 (Production)	Value	Unit
P_{inj}	-	Bar
P_{prod}	30	Bar

Stage 3 (H_2 Injection)	Value	Unit
P_{inj}	100	Bar
P_{prod}	-	Bar

Stage 4 (H_2 Production)	Value	Unit
P_{inj}	-	Bar
P_{prod}	30	Bar

Table 4.3.7: Injection and production pressure in the base cyclic storage scenario

4.3.6. Sensitivity Analysis

Using the homogeneous reservoir as a base scenario, different input parameters have been altered to check the effect on the overall cyclic storage efficiency of the reservoir. This is done looking at the following parameters:

- Dimension ratio of the reservoir
- Injection and Production pressure
- Time scale

By varying the dimensions of the reservoir, the effect of the efficiency of the storage cycles are investigated. By executing this analysis the effect of different ratios of the geometry of the reservoir can be seen.

Case	**LxW [m]**	**H [m]**	
Base Case	750x750	90	
Scenario A	2000x2000	90	
Scenario B	2000x2000	45	

Table 4.3.8: Reservoir dimensions assigned in scenario A and B

In order to check to impact of injection and production pressure on the cycle efficiency, a separate analysis is performed. This is done by applying different pressure regimes to the seasonal storage stages. The net difference between injection and production pressure is both doubled and halved compared to the base scenario. Therefore, the pressure difference of 70 bars used in the base scenario is now shifted to respectively 35 bars and 140 bars difference.

The following reservoir states have been assigned for each stage during the cyclic storage scenario:

Stage 1 (Injection)	Value	Unit
P_{inj}	170	Bar
P_{prod}	-	Bar

Stage 2 (Production)	Value	Unit
P_{inj}	-	Bar
P_{prod}	30	Bar

Stage 3 (H_2 Injection)	Value	Unit
P_{inj}	170	Bar
P_{prod}	-	Bar

Stage 4 (H_2 Production)	Value	Unit
P_{inj}	-	Bar
P_{prod}	30	Bar

Table 4.3.9: Injection and production pressure in scenario A

Stage 1 (Injection)	Value	Unit
P_{inj}	65	Bar
P_{prod}	-	Bar

Stage 2 (Production)	Value	Unit
P_{inj}	-	Bar
P_{prod}	30	Bar

Stage 3 (H_2 Injection)	Value	Unit
P_{inj}	65	Bar
P_{prod}	-	Bar

Stage 4 (H_2 Production)	Value	Unit
P_{inj}	-	Bar
P_{prod}	30	Bar

Table 4.3.10: Injection and production pressure in scenario B

5

Hydrodynamic Behaviour in a 2D Reservoir

In this chapter the results for the 2D simulation are described and interpreted. In order to safely inject H_2 into a depleted gas reservoir, knowledge of the displacement behaviour is essential prior to the operation. The hydrodynamic behaviour of H_2 will be analyzed during the injection phase which corresponds with the previously mentioned stage 3. In the following scenarios the same fluid parameters of the homogeneous H_2 - N_2 and H_2 - N_2 - CH_4 displacement scenarios are used. An overview of this can be found in Table 4.3.1 and Table 4.3.2.

5.1. Displacement in a Homogeneous 2D reservoir

In the following scenarios a homogeneous 2D box reservoir reservoir is used to clearly visualize the displacement of H_2 in contact with another gaseous mixture. The properties of the homogeneous reservoir are corresponding to those listed in Table 4.3.3.

5.1.1. H_2 - N_2 - Displacement

The H_2 - N_2 case simulates the process in which H_2 displaces the cushion gas N_2. The simulation runs for 100 days. At this point the whole reservoir has been cleared of the N_2 component and is filled with 100% H_2. The following figures show the saturation of H_2 in the reservoir at $t = 10$ days and $t = 30$ days.

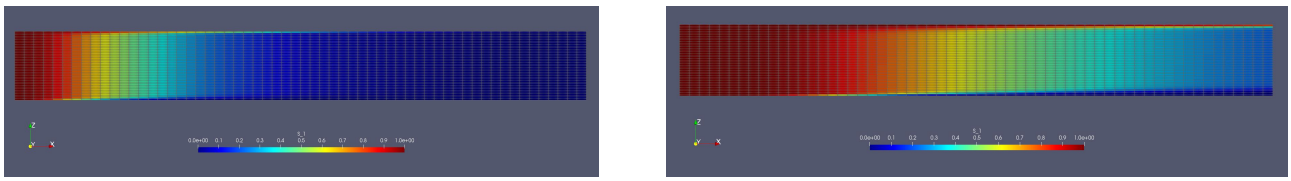

Figure 5.1.1: H_2 displacing N_2 in a homogeneous 2D reservoir after 10 days (left) and 30 days (right)

The resulting simulations show the effect of gravity between the H_2 and N_2 component within the gas phase. Since the permeability in all directions is the same, the lighter H_2 component within the gas phase can easily rise above the initially in place N_2 component. The previously described effect of gravity override is substantiated in this visualization.

5.1.2. Gravity Number Analysis

The ratio between the viscous forces and buoyancy forces is considered to be in advantage of the buoyancy forces causing a change in the displacement front over time. This observation is checked by calculating both the dimensionless gravity numbers N and γ at the interface of the both components. The interface is analyzed a $t = 10$ days. From Equation 3.13, it becomes clear that N is dependent of r_c which represents the characteristic distance from the injection well horizontally to the the interface. Therefore, from bottom to top of the reservoir, r_c will gradually increase looking at the position of the interface in Figure 5.1.1. Due to the curvature of the interface it is evident that the value for N will also vary along the interface of the H_2 and N_2 component. In contrast to N, the parameters used to calculate γ remain constant throughout the simulation. This makes γ a more suitable number to describe the average ratio

between gravitational and viscous forces. In order to describe the ratio of the forces including compressibility and position of the interface for pure H_2, the gravity number N is used.

Using Equation (3.11), the mean gravity number N is 2.09 and increases simultaneously when the characteristic the distance of the interface to the injection well is increased. This makes sense since the gravitational forces are in vertical direction. In proximity to the injection well, the horizontal viscous forces are dominant decreasing the gravity number.

Gravity Number	Value	Dominant Forces
γ	1.13	Comparable
N - mean	2.09	Slightly gravitational
N - near well bore	1.17	Comparable
N - away from well	5.55	Gravitational

Table 5.1.1: Characterization of dominant forces for H_2 - N_2 scenario

The dominant forces are characterized as either viscous, comparable of gravitational according to Table 3.5.1. From Table 5.1.1, it is proven that during the displacement of N_2 by injection of H_2 in a homogeneous horizontal reservoir, gravitational forces are dominant over viscous forces. In the appendix the relation between gravity number and distance from the well is analyzed.

Since under actual reservoir conditions, the horizontal permeability is often found to be significantly greater than the vertical permeability component, a first alteration to the permeability tensor K_{xyz} is implemented. Therefore, in the following simulation, the vertical permeability component (K_z) is reduced from 283 mD to 32 mD.

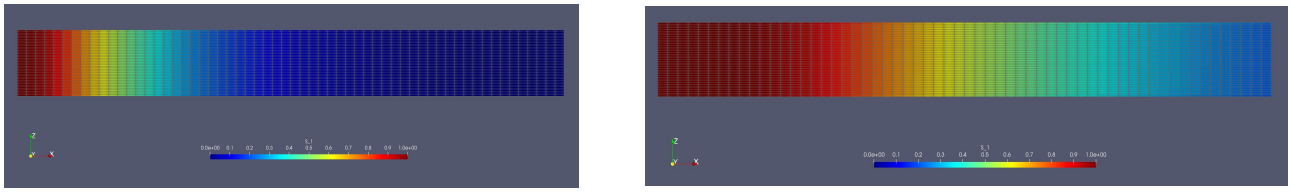

Figure 5.1.2: H_2 displacing N_2 in a homogeneous 2D reservoir with reduced K_z after 10 days (left) and 30 days (right)

Clearly, the ratio between the viscous and buoyancy forces has shifted in favor of the viscous forces. Due to a decrease in vertical permeability by a factor 10, the gravitational forces upward have also been reduced. This makes gravity override much harder to occur leading to stable displacement of H_2 in the horizontal direction.

Gravity Number	Value	Dominant Forces
N - mean	$5.6 \cdot 10^{-3}$	Viscous

Table 5.1.2: Average value of N after reduction in K_z in H_2- N_2 scenario

This is confirmed by looking at the resulting gravity number for the reduced K_z case. Compared to the previous simulation the value for N has decreased significantly meaning that the ratio of the viscous and gravitational forces has shifted in favor of the viscous forces.

5.1.3. H_2 - N_2 - CH_4 Displacement

In the following scenario the same homogeneous 2D reservoir is used. In this case the residual gas is considered to be an ideal mixture of 80% N_2 and 20 %CH_4. The injected gas is again 100% H_2. The simulation time is again set at $t = 100$days. For the following simulation the fluid parameters listed in Table 4.3.2 have been used [28][41]. Noticeable compared to the previous simulations fluid parameters is that the injected H_2 gas will now displace a less dense and less viscous gas compared to pure N_2. Also, the overall compressibility factor of the residual has deceased due to the presence of CH_4. The following figures show the saturation of H_2 in the reservoir at $t = 10$ days and $t = 30$ days.

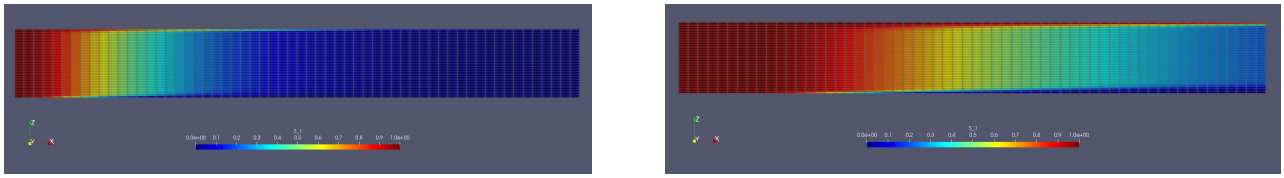

Figure 5.1.3: H_2 displacing N_2 - CH_4 in a homogeneous 2D reservoir after 10 days (left) and 30 days (right)

The resulting simulation again shows the effect of gravity during displacement of H_2 towards the N_2-CH_4 mixture that is initially in place. However, during the same moments in time, the H_2 component has progressed much further compared to the H_2-N_2 case. It seems that the combination of relatively lower density and viscosity values is more favorable for H_2 to be transport in the reservoir.

Gravity Number	Value	Dominant Forces
γ	1.43	Slightly Gravitational
N - mean	1.59	Slightly Gravitational
N - near well bore	1.09	Comparable
N - away from well	4.15	Gravitational

Table 5.1.3: Characterization of dominant forces for H_2 - N_2 - CH_4 scenario

The ratio between the viscous forces and buoyancy is again considered to be in advantage of the buoyancy forces causing a change in the displacement front over time. However, the quantitative difference is analyzed using the gravity number again. Compared to the H_2-N_2 case the value of N has decreased.

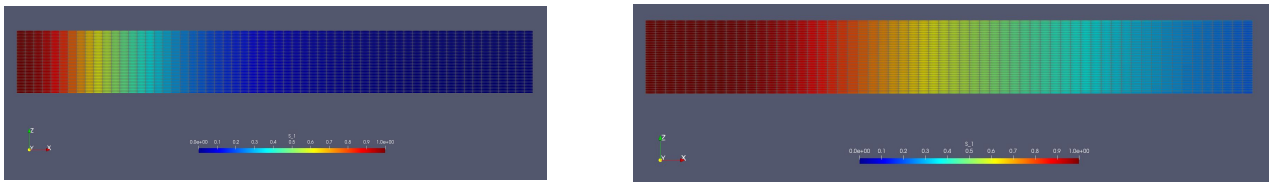

Figure 5.1.4: H_2 displacing N_2 - CH_4 in a homogeneous 2D reservoir with reduced K_z after 10 days (left) and 30 days (right)

Again, the alteration to the permeability tensor K_{xyz} is implemented. Reducing the vertical permeability component (K_z) is from 283 mD to 32 mD. Likewise, the ratio between the viscous and buoyancy forces has again shifted in favor of the viscous forces making gravity override harder to take place. The effect of reducing the vertical permeability component leads to a more stable displacement of H_2 in the horizontal direction. The gravity number shows a slight difference compared to the H_2- N_2 - reduced K_z case.

Mean Gravity Number- N	Value	Dominant Forces
H_2- N_2 - reduced K_z	$5.6 \cdot 10^{-3}$	Viscous
H_2- N_2 - CH_4 - reduced K_z	$4.2 \cdot 10^{-3}$	Viscous

Table 5.1.4: Average value of N after reduction in K_z in H_2- N_2 - CH_4 scenario

The resulting mean N for both cases is listed in Table 5.1.4 The results show that the mean N has decreased the most in the H_2- N_2 - CH_4 - reduced K_z scenario.

5.2. Production Efficiency of H_2

Next, an analysis is performed in terms of production efficiency of H_2. The previous simulations have all been performed until the whole of the 2D reservoir is saturated with H_2 gas. Therefore, it is possible to describe which case shows the most efficient displacement of the residual gas over time. From the previously shown results of the respective simulations, it is visible that the displacement front at $t = 10$ days and $t = 30$ days in the H_2 - N_2-CH_4 scenario has progressed significantly further compared to the H_2 - N_2 scenario. This implies H_2 can more easily displace the mixture of N_2 - CH_4 than pure N_2 gas.

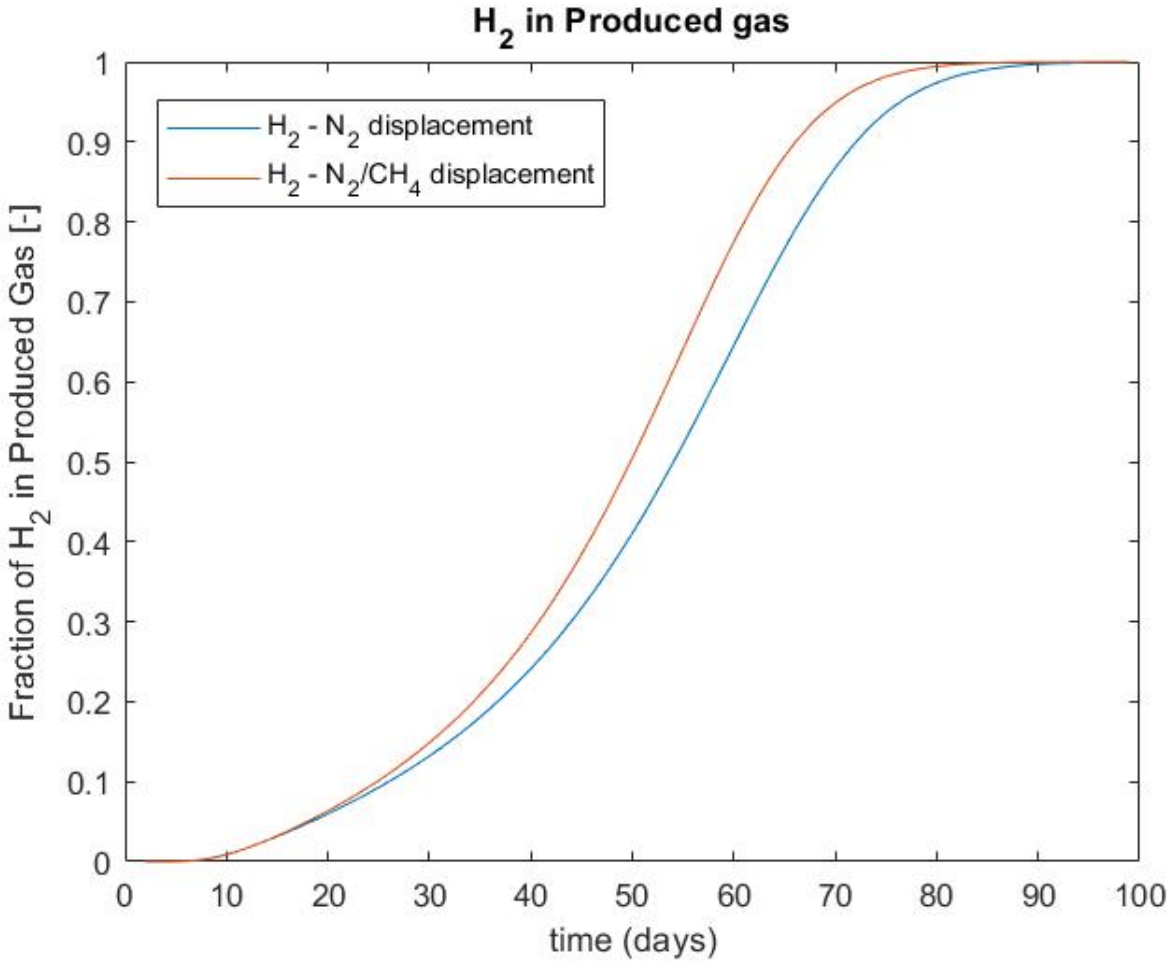

Figure 5.2.1: Fraction of hydrogen produced in both cases for a homogeneous reservoir

This implication is confirmed by looking at Figure 5.2.1. A visualization of the fraction of H_2 present is the production well is shown over a time span of 100 days for both the H_2 - N_2 scenario and the H_2 - N_2-CH_4 scenario. The result clearly shows that after roughly $t = 25$ days an increase in H_2 production is witnessed in the H_2 - N_2-CH_4 scenario. This proves that H_2 can more easily displace a mixture of N_2-CH_4 which could have a positive effect on the overall efficiency of the injection and production cycle of storing H_2 in depleted gas reservoirs.

5.3. Displacement in a heterogeneous 2D Reservoir

For the following scenarios, a 2D slice of the heterogeneous 3D dataset of the Delft Sandstone aquifer is used. Initially, the simulation time is kept the same as in the homogeneous simulations at $t = 100$ days.

5.3.1. H_2 - N_2 Displacement

The same fluid parameters of the homogeneous H_2 - N_2 and H_2 - N_2 - CH_4 displacement scenarios are used. An overview of this can be found in Table 4.3.1. and Table 4.3.2. The reservoir specific properties have logically changed using the heterogeneous reservoir data set. In Table 4.3.5 an overview is given of all the properties used to perform the heterogeneous 2D simulation.

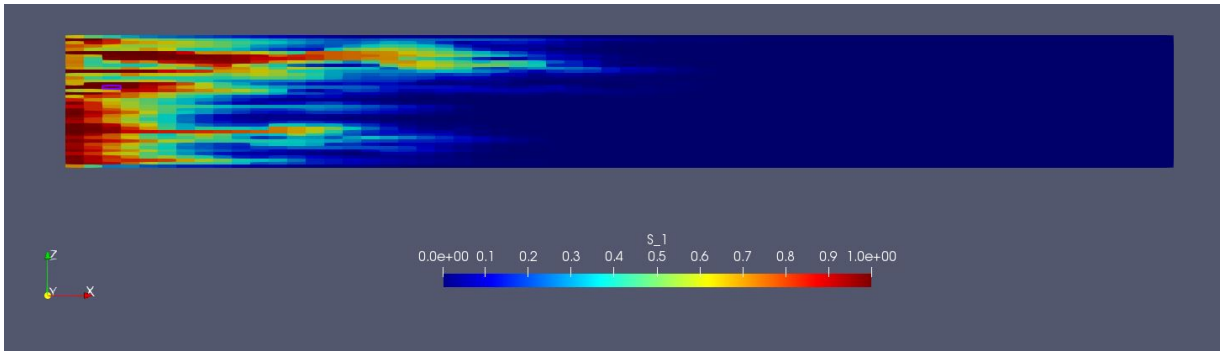

Figure 5.3.1: H_2 displacing N_2 in a heterogeneous 2D reservoir at t=10 days

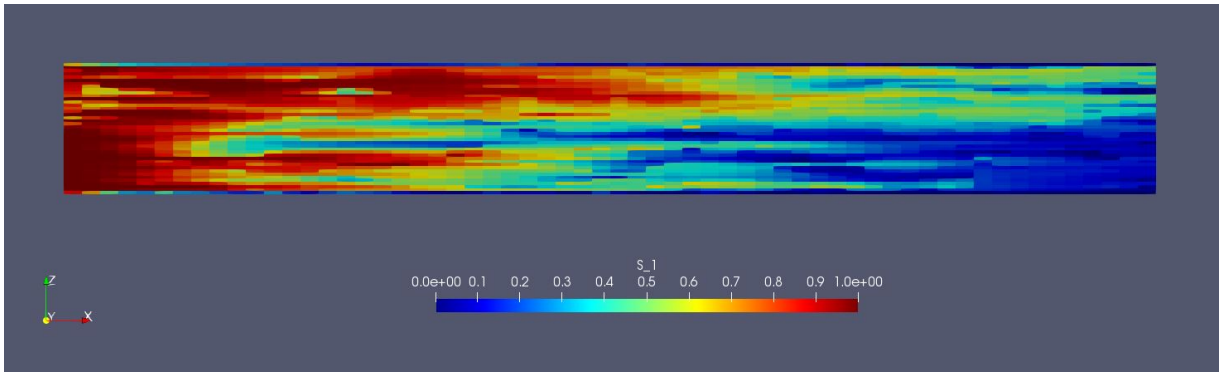

Figure 5.3.2: H_2 displacing N_2 in a heterogeneous 2D reservoir at t=30 days

The above results visualize the saturation of H_2 within the reservoir at different time steps. The effect of preferential pathways created by high perm streak is clearly visible. The high perm streaks cause the net-gross ratio (N/G) to be highly reduced. Therefore, the injected H_2 will mainly be transported through the high perm streaks. Consequently, this reduces the effective volume in the reservoir through which H_2 can effectively flow.

5.3.2. H_2 - N_2 - CH_4 Displacement

In the following section, the displacement of H_2 towards the mixture of N_2 - CH_4 in the heterogeneous reservoir is visualized.

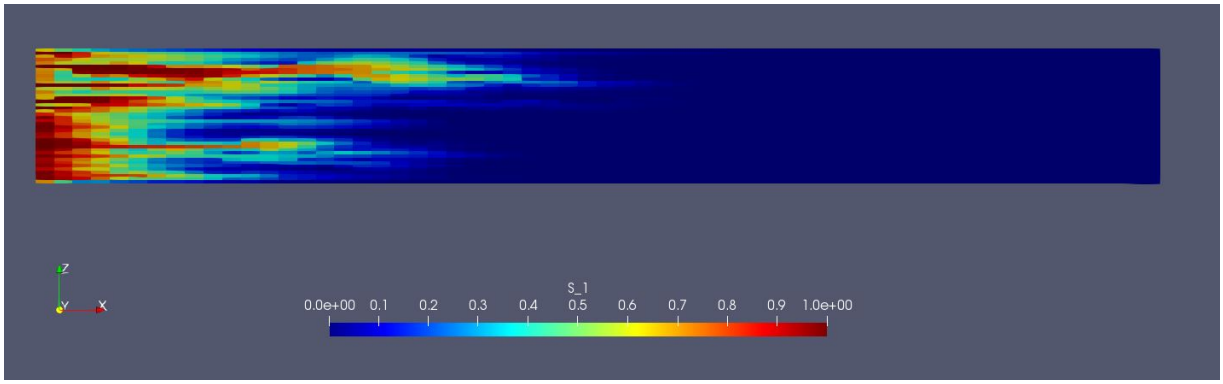

Figure 5.3.3: H_2 displacing N_2-CH_4 in a heterogeneous 2D reservoir at t=10 days

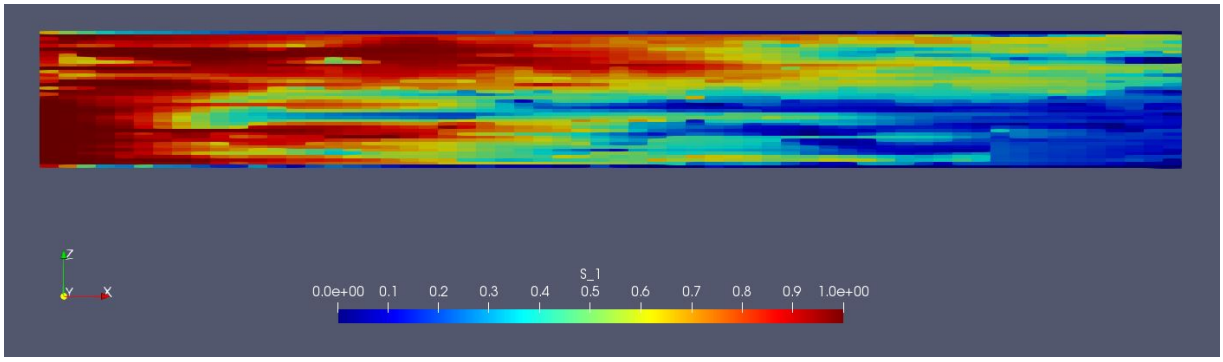

Figure 5.3.4: H_2 displacing N_2-CH_4 in a heterogeneous 2D reservoir at t=30 days

As can be seen from Figure 5.3.3 and Figure 5.3.4, there are not too much differences observed compared to the H_2 - N_2 case. The relative effect in hydrodynamic behaviour is significantly reduced due to the heterogeneity that is introduced to the reservoir. In term of produced fraction of H_2, a more clear difference between both scenarios can be distinguished.

5.3.3. Production Efficiency of H_2

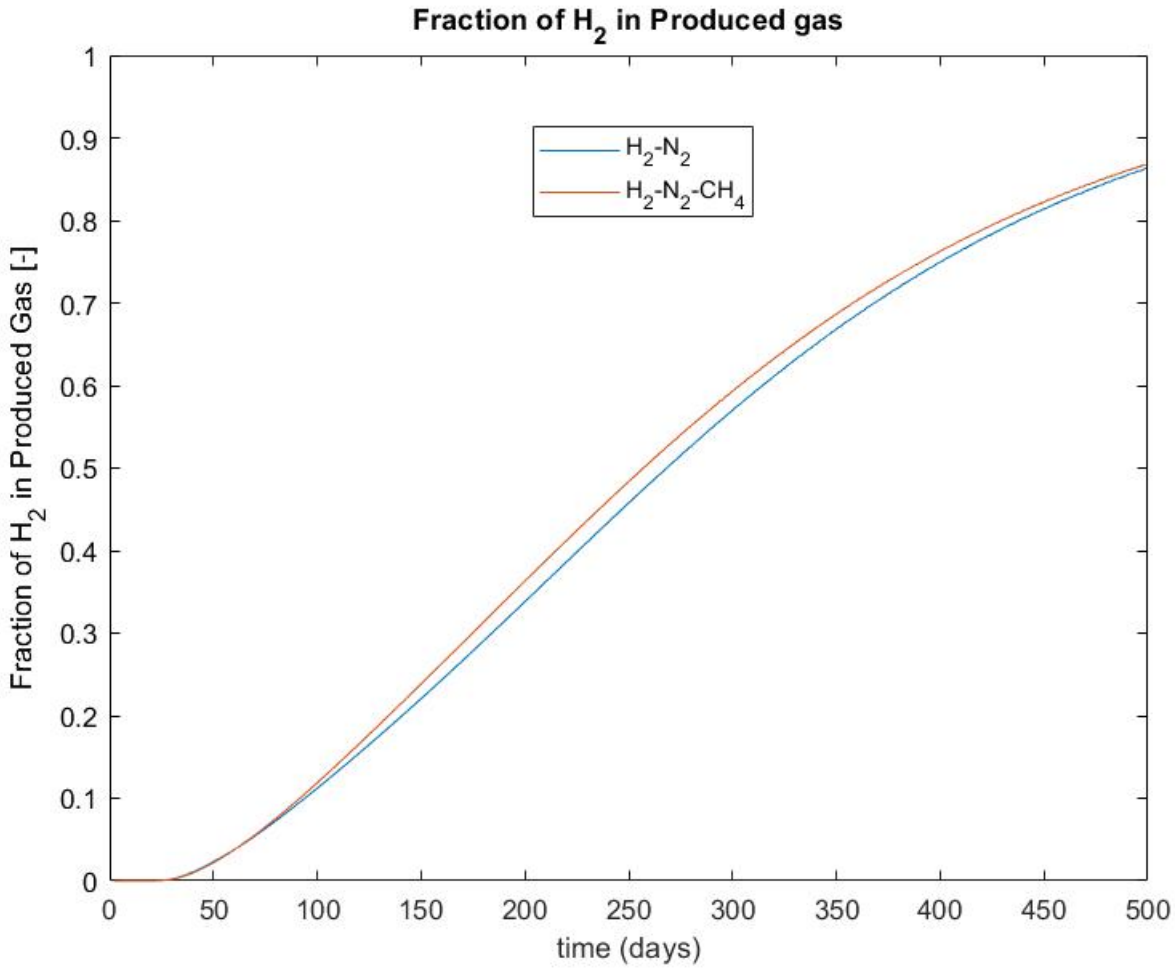

Figure 5.3.5: Fraction of hydrogen produced in both cases for a heterogeneous reservoir

In Figure 5.3.5 the resulting fraction of H_2 in the produced gas has been visualized for both the case where H_2 displaces N_2 and when H_2 displaces N_2-CH_4. It is clear that at $t = 100$ days, for both cases, just over 10% of H_2 can be extracted from the produced gas. Compared to the homogeneous case, this is a drastically decrease in efficiency. In order to improve the fraction of H_2 in the produced gas at the end of simulation time, the decision is made to increase the simulation time until the 'successful' percentage of 82% of H_2 is reproduced [13]. The simulation time is stopped afterwards since it will take a significant longer time period to obtain a 100% fraction of H_2 in the producing well. In both cases, the simulation time is increased to 500 days. For both the H_2 - N_2 case and the H_2 - N_2 - CH_4 case, the successful production percentage of 82% of H_2 in the produced gas can be observed at respectively $t = 458$ and $t = 466$ days. This is significantly later than when the same simulation is performed on the homogeneous reservoir.

Also, it is again clear that during the H_2 - N_2 - CH_4, during most of the simulation time, a higher fraction of H_2 can be found in the producing well compared to the H_2 - N_2 scenario. Due to the increase in simulation time however, this effect has become relatively small compared to the homogeneous case. It has become clear that in order to define the performance of depleted gas reservoir for the storage of H_2, the amount of time that necessary to reproduce the injected H_2 should be thoroughly analyzed when comparing the results.

6

Seasonal storage performance in a 3D Reservoir

In order to simulate the seasonal storage process of H_2 in an underground reservoir, the most realistic results can be obtained when cyclic simulations can be implemented and performed by the reservoir simulator.

6.1. Homogeneous Box Reservoir

For the homogeneous case, the same reservoir properties of a Dutch depleted gas reservoir are used as in Chapter 5. Each of the four stages each last for 100 days.

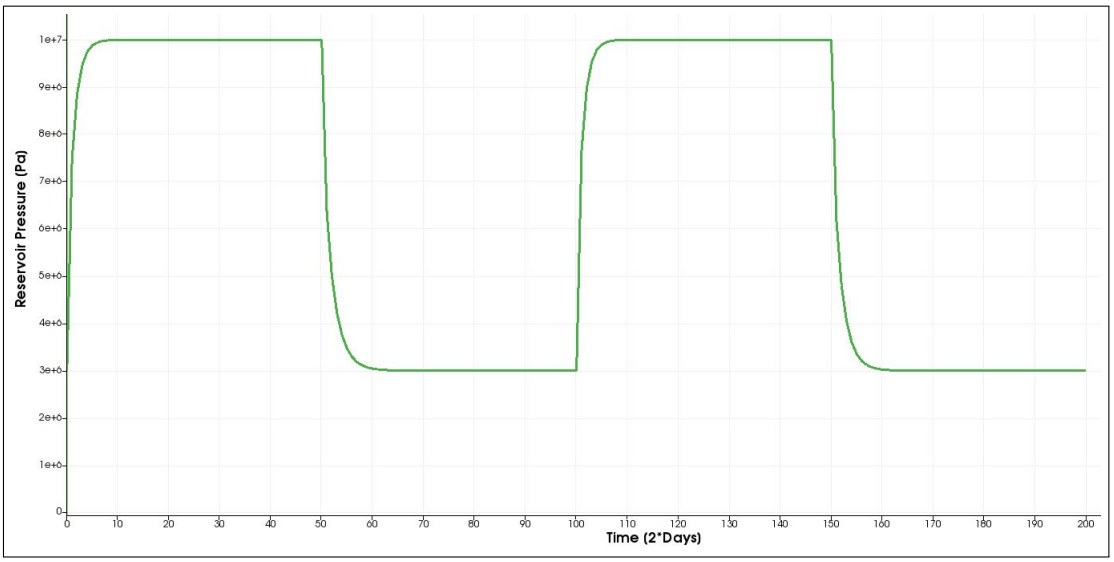

Figure 6.1.1: Reservoir pressure vs. time in a homogeneous box reservoir

The pressure regime in the reservoir, visualized in Figure 6.2.1, throughout the 400 days of simulation shows the previously described simulation strategy (Note that the time steps of the simulations are each 48 hours). The increasing pressure regimes show the stages where H_2 is injected in the reservoir whereas the pressure declines are caused by the production of gas from the reservoir. The efficiency of the injection and production cycles can be described by the fraction of H_2 that remains inside the reservoir after production.

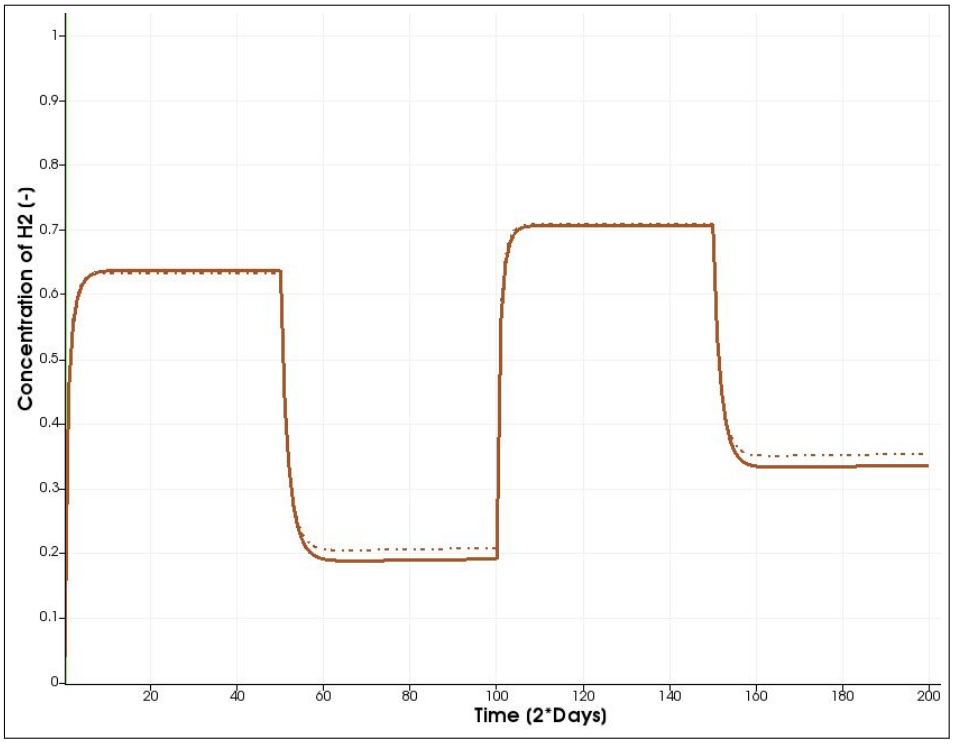

Figure 6.1.2: Concentration of H_2 present in a homogeneous reservoir
- - - = H_2 - N_2
—— = H_2 - N_2 - CH_4

Using the aforementioned strategy the efficiency of two subsequent storage cycles are analysed. For both the case where H_2 is displacing N_2 or a mixture of $N_2 - CH_4$ the amount of produced H_2 is compared to the injected volume. This is visualized in Figure 6.1.2

From both Figure 6.1.1 and Figure 6.1.2 two main observations can be described that are directly linked to the efficiency of cyclic H_2 storage in porous media.

- Comparing both cases, using the same well strategy, a slight difference is observed in the amount of H_2 that that can be injected and reproduced. Similar to the 2D results, a higher fraction of H_2 can be produced in the H_2 - N_2 - CH_4 scenario.
- For both cases, at the end of the second cycle and using the same well strategy, the amount of H_2 left in the reservoir has significantly increased compared to the first cycle.

In theory, the total amount of H_2 that is injected could be reproduced using the same time intervals and same pressure difference. The efficiency per full cycle is therefore calculated as follows:

$$\eta_{stage_x} = \frac{Net\ H_{2\ inj}}{Net\ H_{2\ prod}} \tag{6.1}$$

H_2 **in Reservoir**	H_2-N_2		H_2-N_2-CH_4	
Time (days)	*t=100*	*t=200*	*t=100*	*t=200*
Fraction of reservoir saturated by H_2 in Cycle 1	63.2%	20.7%	63.7%	19.0%
Total efficiency of Cycle 1	67.2%		70.2%	
Time (days)	*t=300*	*t=400*	*t=300*	*t=400*
Fraction of reservoir saturated by H_2 in Cycle 2	70.8%	35.4%	70.6%	33.5%
Total efficiency of Cycle 2	70.6%		71.9%	

Table 6.1.1: Efficiency of multiple cycles of H_2 storage in a homogeneous box reservoir

The corresponding efficiency values of the homogeneous box are listed in Table 6.1.1.

In the H_2-N_2 scenario, a maximum efficiency of **67.2**% is obtained in the first cycle. In the H_2-N_2-CH_4, a higher maximum efficiency is reached i.e.**70.2**%. For both scenarios, it is clear that the cycle efficiency increases slightly in the subsequent cycle. This increase in efficiency can most likely be linked to the higher initial saturation of H_2 at the start of the second cycle

6.2. Heterogeneous Box Reservoir

In the heterogeneous case, the full 3-dimensional dataset of the Delft Sandstone reservoir has been used.

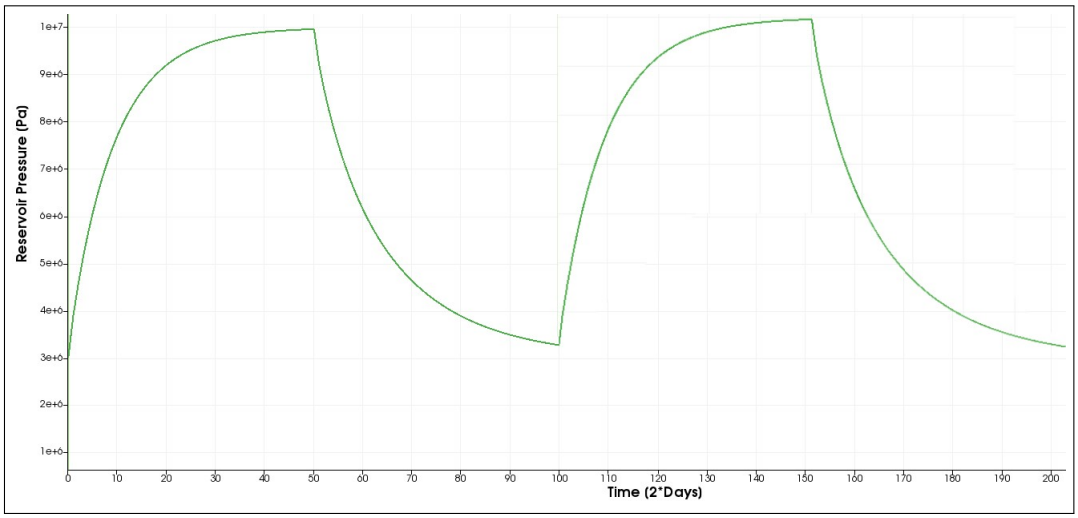

Figure 6.2.1: Reservoir pressure vs. time in a heterogeneous box reservoir

When the pressure regime is compared with the homogeneous 3D case, it is clear to see that it takes a significant amount of time longer for the average reservoir pressure to reach the upper constraint of 100 bars. Where this occurred at roughly $t = 20$ days in the homogeneous case, this reservoir pressure is now reached at the end of the first stage i.e. $t = 100$ days. This delay already indicates that in the heterogeneous case more time is necessary to saturate the reservoir with H_2. Also, in the production stage, it is noticeable that after 100 days of production, the lower constraint of 30 bars has not yet been reached.

The effect of the displacement efficiency of H_2 towards different cushion gasses is even more reduced in the heterogeneous case. The saturation of H_2 within the reservoir almost follows the same curve for both scenarios.

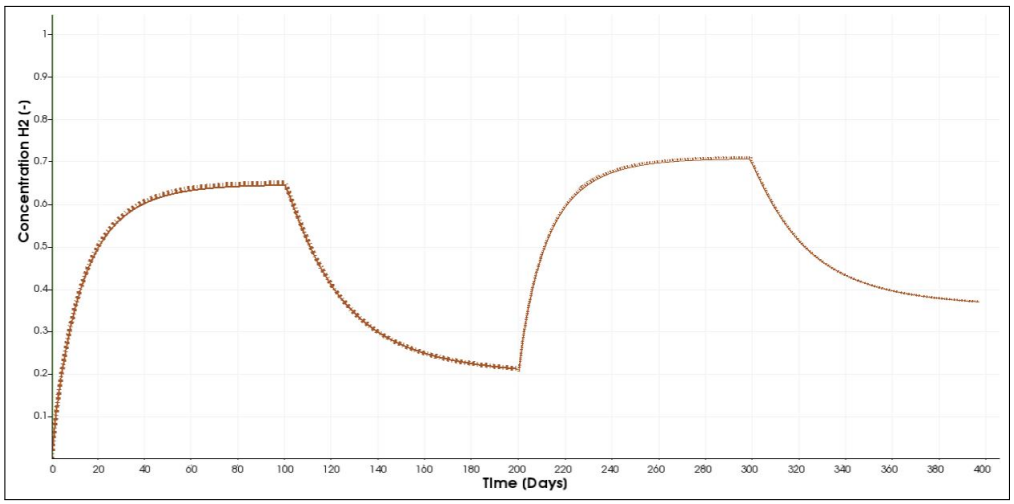

Figure 6.2.2: Concentration of H_2 present in the heterogeneous reservoir
- - - = H_2 - N_2
—— = H_2 - N_2 - CH_4

The same well strategy as for the homogeneous case leads to the following values in terms of efficiency per storage cycle:

H_2 **in Reservoir**	H_2-N_2		H_2-N_2-CH_4	
Time (days)	*t=100*	*t=200*	*t=100*	*t=200*
Fraction of reservoir saturated by H_2 in Cycle 1	63.2%	22.1%	63.7%	22.0%
Total efficiency of Cycle 1	65.0%		65.4%	
Time (days)	*t=300*	*t=400*	*t=300*	*t=400*
Fraction of reservoir saturated by H_2 in Cycle 2	71.1%	38.4%	70.5%	38.0%
Total efficiency of Cycle 2	67.6%		67.9%	

Table 6.2.1: Efficiency of multiple cycles of H_2 storage in a heterogeneous box reservoir

The same observations are seen on a relatively smaller scale when applying an heterogeneous reservoir to this cyclic storage configuration. The H_2-N_2-CH_4 scenario appears to be slightly more efficient compared to H_2-N_2 scenario. However, the heterogeneity reduces the absolute difference between these scenarios. Again, a small increase in both scenarios is witnessed in the second storage cycle compared to the first cycle. Another important observation is the time it takes per stage to reach the maximum concentration reached in either the injection or production stage. Since the upper and lower pressure constraints of the injection and production wells are reached at a later moment during each stage, the wells can both inject and produce for a longer period of time. Compared to the homogeneous reservoir, the cycle efficiency reaches comparable values in the heterogeneous scenario. However, it takes a significantly longer to reach this level of efficiency compared to the homogeneous scenario. The noticeable difference in efficiency between the H_2-N_2 scenario and the H_2-N_2-CH_4 scenario that was encountered in the homogeneous reservoir, diminished in the heterogeneous reservoir simulations.

7

Sensitivity Analysis

Using the homogeneous reservoir as a base scenario, different input parameters have been altered to check the effect on the overall cyclic storage efficiency of the reservoir. This is done by looking at the following parameters:

- Dimension ratio of the reservoir
- Injection and Production pressure
- Time scale

7.1. Reservoir Dimensions

By varying the dimensions of the reservoir, the effect of the efficiency of the storage cycles are investigated. The results of this analysis shows what the effect of the dimensions of the reservoir is on the overall cycle efficiency.

H_2 **in Reservoir**	Base		Scenario A		Scenario B	
Time (days)	*t=100*	*t=200*	*t=100*	*t=200*	*t=100*	*t=200*
Fraction of reservoir saturated by H_2 in Cycle 1	63.7%	19.0%	63.7%	16.4%	63.7%	16.6%
Total efficiency of Cycle 1	70.2%		74.3%		74.5%	
Time (days)	*t=300*	*t=400*	*t=300*	*t=400*	*t=300*	*t=400*
Fraction of reservoir saturated by H_2 in Cycle 2	70.6%	33.5%	69.3%	27.5%	69.5%	27.6%
Total efficiency of Cycle 2	71.9%		79.0%		79.2%	

Table 7.1.1: Efficiency of multiple cycles of H_2 storage using different reservoir dimensions

Increasing the length & width of the reservoir while maintaining the the same reservoir height leads already leads to a rise in cycle efficiency. Subsequently in Scenario B, the height of the reservoir is decreased, making the reservoir more thin and elongate. The effect of adjusting the reservoir has an almost negligible effect on the cycle efficiency. Important to note is that in scenario A and B the constraint of respectively 100 bar injection pressure and 30 bars production pressure are reached relatively later in each phase compared to the base scenario. In other words, the overall cycle efficiency increases but the time necessary to fully inject and produce from the reservoir has simultaneously increased in both scenario A and B. Overall, an significant increase of maximum 7.3% efficiency is achieved in scenario B compared to the base scenario.

7.2. Injection & Production Pressure

The higher and lower pressure difference applied to the reservoir leads to the following concentration of H_2 present in the reservoir over time.

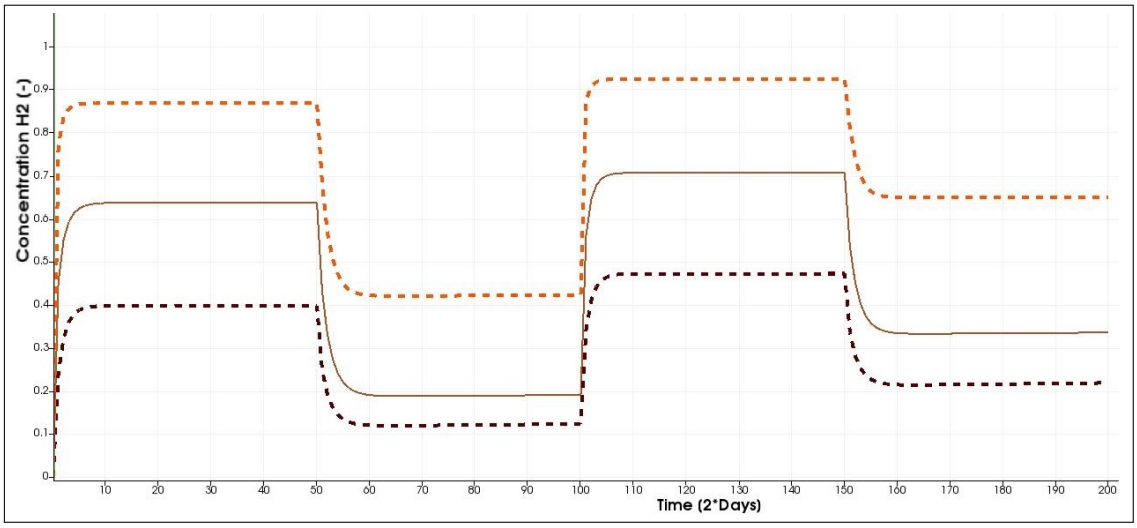

Figure 7.2.1: Concentration of H_2 present in the reservoir
- - - = Scenario A
- - - = Scenario B
—— = Base

H_2 **in Reservoir**	Base		Scenario A		Scenario B	
Time (days)	*t=100*	*t=200*	*t=100*	*t=200*	*t=100*	*t=200*
Fraction of reservoir saturated by H_2 in Cycle 1	63.7%	19.0%	86.9%	42.3%	39.7%	12.3%
Total efficiency of Cycle 1	70.2%		51.3%		69.0%	
Time (days)	*t=300*	*t=400*	*t=300*	*t=400*	*t=300*	*t=400*
Fraction of reservoir saturated by H_2 in Cycle 2	70.6%	33.5%	92.4%	64.9%	47.2%	21.8%
Total efficiency of Cycle 2	71.9%		54.9%		72.7%	

Table 7.2.1: Efficiency of multiple cycles of H_2 storage using different injection and production pressures

From the sensitivity analysis it becomes clear that introducing a higher pressure difference in the same time span initially leads to a higher concentration of H_2 present in the reservoir, but significantly deceases the cycle efficiency. This means that relatively more H_2 can be injected but less H_2 is retrieved. By decreasing the pressure difference by 50% a slightly higher cycle efficiency is achieved. However, a maximum of just 47.2% of the reservoir is saturated with H_2 in the second cycle. This means that almost half of the reservoir capacity is not utilized during this scenario.

7.3. Time Scale Effect

The efficiency of the storage cycles in the base scenario was calculated for time periods of 100 days per injection or production stage. Now the effect of timescale is analyzed by means of:

- Scenario A: Decreasing the cycle length to 2 months, i.e. 1 month of injection followed by 1 month of production
- Scenario B: Extending the cycle length to a full year i.e. 183 of injection followed by 100 days of production

The results of the simulations are listed in table:

H_2 **in Reservoir**	Base		Scenario A		Scenario B	
Time (days)	*t=100*	*t=200*	*t=30*	*t=60*	*t=183*	*t=366*
Fraction of reservoir saturated by H_2 in Cycle 1	63.7%	19.0%	63.5%	19.2%	63.9%	18.6%
Total efficiency of Cycle 1	70.2%		69.7%		70.8%	
Time (days)	*t=300*	*t=400*	*t=90*	*t=120*	*t=549*	*t=732*
Fraction of reservoir saturated by H_2 in Cycle 2	70.6%	33.5%	70.2%	33.7%	73.5%	32.3%
Total efficiency of Cycle 2	71.9%		71.6%		75.0%	

Table 7.3.1: Efficiency of multiple cycles of H_2 storage using different duration for injection and production stages

It is clear to see that the cycle efficiency in the scenario A, where the length per cycle has been decreased, shows only a little decrease in efficiency. This is because most of the injected H_2 is reproduced in the the first 15 days of the production stage. Afterwards, the production rate per day severely decreases since the threshold production pressure of 30 bars has been reached. Vice versa, during the injection of H_2 the upper constraint of 100 bars for the injection pressure is also reached after roughly 15 days of of injection. By extending the time per stage, as is done in scenario B, the efficiency of the storage cycles is increased. Since slightly more H_2 can be injected and produced over a longer time period, a higher overall efficiency is achieved. However, comparable cycle efficiency can already be achieved by using the cycle length as described in scenario A.

8

Conclusion

The objective of this research was to asses if seasonal H_2 storage is technically feasible in Dutch depleted gas reservoirs. Firstly, the need for seasonal storage for 2050 in The Netherlands was quantified. Based on the reservoir specific properties from the portfolio of Dutch gas reservoir a first analysis was made, identifying the need for gas reservoir capacity instead of other suitable geological formations. Then, based on literature, various complexities and issues with UHS in depleted gas reservoirs were addressed and quantified. Subsequently, using the DARSim2 reservoir simulator, the hydrodynamic behaviour of H_2 in porous media was described according to the dimensionless gravity number. Lastly, additions were made to DARSim2 simulator which made it possible to perform cyclic simulations investigating the efficiency of retrieving the injected H_2 in the reservoir. By means of a sensitivity study, the effect of different input parameters of this model were analysed. The conclusions of this thesis are presented by answering the different sub-questions.

- *What is the necessary capacity for H_2 that needs to be met in order to define this storage technique as feasible?*

By defining a minimal need of 16 TWh for seasonal H_2 storage in The Netherlands in 2050, a strategy was proposed quantifying the need for storage specifically in depleted gas reservoirs in The Netherlands. Firstly, the need for the storage of H_2 was quantified for 2050. Then, based on the effective storage capacity of the Dutch subsurface, it became clear that 456 TWh of H_2 could be stored theoretically in 321 salt caverns and 140 gas reservoirs. Due to the relatively higher efficiency and limited safety risks, salt caverns have the priority compared to the other potential formations suitable for H_2 storage. Based on both policy related scenarios and possible meteorological conditions, a minimal need for H_2 storage in 2050 was defined at 16 TWh [23]. Concluding, by constructing 90 caverns in 2050, a minimal need for 3.9 TWh of H_2 storage in Dutch gas reservoirs was identified.

- *What losses of H_2 can be expected during the first and subsequent storage cycles?*

Literature shows that the losses of potential energy due to the loss of H_2 can be divided into different segments. Firstly, a loss of H_2 was to be expected due to the interaction of H_2 with the reservoir rock, leading to geochemical reactions. Experimental studies showed that typical sandstone abundant minerals as K-feldspars and quartz will not be highly reactive with the H_2 gas under subsurface conditions [7]. Therefore, the losses by geochemical conversion will be minimal. Geochemical effects could induce porosity changes leading to a maximum decrease of 0.21% [22]. The dissolution of H_2 will also not account for great amounts of H_2 losses during subsurface storage. The solubility of H_2 is minimal at around 100^oC which is roughly in the range of the temperature of many Dutch gas reservoir. Therefore, the respective losses will be minimal and are predicted between 0.88 - 2% of the total injected H_2 volume [13][32]. The losses by dissolution can be seen as a one-time loss since after the first injection cycle the liquid in the reservoir rock is saturated with the dissolved H_2. The diffusion of H_2 through the caprock is an area of research that no field studies with 100% H_2 have been conducted for so far. Therefore, from numerical simulation studies, the losses by diffusion through the caprock are estimated up to 6% [13]. The mixing of H_2 in residual gasses such as cushion gas is likely to lead a loss of 3% in the first cycle. During subsequent cycles this loss will be lower and eventually decreasing to 1% of the injected volume [43]. Through several microbiological reactions H_2 can also be converted to other molecules leading to the loss of pure H_2 gas. Methanogenesis and SRB are likely to be problematic when there is a noticeable concentration of respectively CO_2 and sulphur present in the reservoir. Potential subsurface storage sites for H_2 in The Netherlands should therefore have a low initial concentration of these molecules. Moreover, the

activity of the microorganisms is limited by choosing reservoirs with a high enough temperature and salinity content in order to make the conditions for the organisms inhabitable [18]. Otherwise, losses up to 50% over a time span of 30 years can be expected [22].

- *How can the hydrodynamic behavior between H_2 and residual fluids be described?*

The displacement of H_2 towards different reservoir fluids was analysed by describing the ratio between the gravitational and viscous forces acting on the gasses. The choice was made to analyse both the displacement of the potential cushion gas (N_2) and an ideal mixture of the cushion gas and residual methane ($N_2 - CH_4$). Using the dimensionless gravity numbers N and γ a quantification could be given in the ratio of gravitational and buoyancy forces that are exerted on the different gas components [27]. In the homogeneous 2D cases a more stable displacement was seen in the H_2-N_2-CH_4 case leading to a higher efficiency during the displacement by H_2. The gravity number analysis showed that the displacement of H_2 with both residual gasses is slightly dominated by gravitational forces in a fully homogeneous reservoir. Reducing the vertical permeability as would be the case in most existing gas reservoirs change the dominating forces to a more viscous displacement. Introducing heterogeneity in permeability and porosity to the 2D reservoir made clear that H_2 is prone to move in the high permeability streaks reducing the efficiency of the displacement. Moreover, the time to fully saturate the 2D reservoir increased by a factor of five, thus decreasing the displacement efficiency significantly.

- *What levels of H_2 storage efficiency can be achieved by utilizing a depleted gas reservoir as storage site?*

By implementing the option to perform cyclic 3D simulations in the original DARSim2 simulator, an analysis was performed on the cycle efficiency during the first and subsequent seasonal storage cycles. By analysing the homogeneous reservoir for both N_2 and $N_2 - CH_4$ as residual gas, it became clear that a slight increase in efficiency was found in the H_2-N_2-CH_4 scenario. Moreover, for all simulations , an increase in cycle efficiency was found in the subsequent storage cycle. For the homogeneous reservoir the highest efficiency that was achieved was 71.9%. By introducing heterogeneity the noticeable difference between the H_2-N_2 and H_2-N_2-CH_4 scenario was decreased. The cycle efficiency decreased by roughly 5%. The most noticeable difference was found looking at the pressure of the reservoir throughout the simulation. In the heterogeneous scenario, the upper constraint of the injection pressure was reached at nearly the end of the injection stage. The lower constraint during the production stage was never reached. In comparison with the homogeneous scenarios, this was a significant change since both the upper and lower pressure constraints were reached within the first 30 days of each stage.

- *What is the impact of the simulation input parameters on the overall efficiency of this technique?*

A sensitivity analysis was performed to validate the results and to analyse the effect of respective input parameters assigned to the 3D cyclic simulations. By increasing the length and width of the reservoir, a maximum increase in cycle efficiency of 7.1% was achieved. Afterwards, the previous reservoir was also decreased in height by 50%. The smaller height of the reservoir lead to a minor addition of 0.2% in cycle efficiency. By doubling the difference in injection and production pressure, a greater volume of H_2 could be stored and produced from the reservoir. However, in terms of net cycle efficiency, this increase in pressure difference had a negative effect on the cycle efficiency. A reduction of 18.9% was the result. Decreasing the net pressure difference by 50% of the injection and production stage had an almost negligible effect on the cycle efficiency. Therefore, the initially used pressure difference of 70 bars showed to be a good range in order to cyclically store H_2 in a depleted gas reservoir. The effect of time scale was analysed by first decreasing the time per stage to one month and afterwards increasing the time per stage to half a year. The effect of reducing the time per stage had a minor negative impact on the cycle efficiency since there was less time to inject and produce from the reservoir. However, increasing the time per stage by 83% only leads to a maximum increase in efficiency of 3.1%. Therefore, the time scale of one month per stage is already sufficient to reach the average cycle efficiency of roughly 70%. From the sensitivity analysis the conclusion was made that the biggest increase in efficiency was increasing the length and width of the reservoir. The greatest reduction in efficiency was achieved by increasing the net pressure difference between the injection and production stage.

Discussion

From literature it became clear that cycle efficiency also depends on multiple independent aspects including the conversion of pure H_2 gas in the reservoir and diffusion through the caprock [19]. These losses were not taken into account when calculating the cycle efficiency. By using the field data of a specific Dutch depleted gas reservoir, an estimation in losses due to the previously mentioned mechanisms could be provided. In terms of simulation methodology a few key assumptions were made that are likely to have a significant impact on the simulation results.

First of all, the gasses were assumed to be immiscible and therefore no mixing between the gasses takes place. This limits the possibilities of transport of the injected H_2 through the porous media. Therefore, the ability of the gas to disperse in the reservoir is limited. This would have a significant impact on the hydrodynamic behaviour of H_2 in contact with other residual gasses which could be described by a change in gravity number for example. Furthermore, no equations of state (EoS) for H_2 were incorporated in the DARSim2 reservoir simulator. This meant that the density was calculated based on linear compressibility of the different gas components.

Also, the viscosity was treated as a constant value in this study, whereas this parameter would also change under different temperature and pressure conditions. The geometry of the reservoir can be seen as the first structural trapping mechanism of H_2. In the simulation a box reservoir with no angle of inclination was assumed. One can imagine that, comparable to natural gas reservoirs, a curved anticlinal shape of the reservoir would make it possible for H_2 to accumulate in a more central region. This would lead to a reduction in lateral spreading of H_2 in the reservoir. Furthermore, it is unlikely that a depleted gas reservoir will have a completely horizontal orientation. The effect of inclination would impact the gravitational forces during the transport of H_2 which could impact the cyclic storage efficiency. The introduction of using differently shaped reservoir could have a significant impact on the overall efficiency of the storage cycles.

Lastly, from Table 1.4.1 the conclusion was drawn that the salt caverns are currently the most safe geological formation for seasonal storage. In order to reduce the risks caused by induced seismicity, the effect of cyclic pressure on sensitive area as nearby faults or compressible overburden layers needs to be further investigated. In order to provide a more detailed study of the overall efficiency of the cyclic storage of H_2 in depleted gas reservoirs, all of the above mentioned subjects need to be taken into account to execute a more accurate analysis of the cycle efficiency.

Bibliography

[1] Jörg Gigler and Marcel Weeda. A programmatic approach for Hydrogen innovations in the Netherlands Hydrogen for the energy transition TKI NIEUW GAS Topsector Energie. (June), 2019.

[2] A. Sainz-Garcia, E. Abarca, V. Rubi, and F. Grandia. Assessment of feasible strategies for seasonal underground hydrogen storage in a saline aquifer. *International Journal of Hydrogen Energy*, 42(26):16657–16666, jun 2017.

[3] Rijkswaterstaat. Dashboard - Energiegebruik - Nederland, 2018.

[4] John Davison, Silvio Arienti, Paolo Cotone, and Luca Mancuso. Co-production of hydrogen and electricity with CO2capture. In *Energy Procedia*, 2009.

[5] Chris Hellinga. Hydrogen-the key to the energy transition. Technical report, 2018.

[6] Shabani B. Moore J. A Critical Study of Stationary Energy Storage Policies in Australia in an International Context: The Role of Hydrogen and Battery Technologies. (9):674, 2016.

[7] Alireza Ebrahimiyekta. Characterization of geochemical interactions and migration of hydrogen in sandstone sedimentary formations : Application to geological storage. page 190, 2017.

[8] Howard B.J. Stone, Ivo Veldhuis, and R. Neil Richardson. Underground hydrogen storage in the UK. *Geological Society Special Publication*, 313:217–226, 2009.

[9] EBN and TNO. Ondergrondse Opslag in Nederland: Technische Verkenning. (November), 2018.

[10] S. Shiva Kumar and V. Himabindu. Hydrogen production by PEM water electrolysis – A review. *Materials Science for Energy Technologies*, 2(3):442–454, dec 2019.

[11] Michael Fischer, Mathew Werber, and Peter V. Schwartz. Batteries: Higher energy density than gasoline? *Energy Policy*, 37(7):2639–2641, jul 2009.

[12] Nick Owen. Roads2Hycom - Fuel Cells and Hydrogen in a Sustainable Energy Economy. *Contrac*, 2009.

[13] RAG Austria, AXIOM Prozesstechnik GesmbH, VERBUND AG, MONTANUNIVERSITÄT LEOBEN, UNIVERSITÄT für Bodenkultur Wien, ENERGIEINSTITUT an der Johannes Kepler Universität Linz. Final Report Programmsteuerung Programmabwicklung. Technical report, RAG Austria, Wien, 2017.

[14] NAM. Gasopslag locaties, 2018.

[15] NLOG. BGM, ALK, NORG, GRK.

[16] CEDIGAZ. Underground Gas Storage in the World – Part 1: Current capacity., 2017.

[17] M. Panfilov. Underground and pipeline hydrogen storage. In *Compendium of Hydrogen Energy*, pages 91–115. Elsevier, 2016.

[18] Netherlands Enterprise Agency. The effects of hydrogen injection in natural gas networks for the Dutch underground storages. page 74, 2017.

[19] Joaquim Juez-Larré, Serge van Gessel, Rory Dalman, Gijs Remmelts, and Remco Groenenberg. Assessment of underground energy storage potential to support the energy transition in the Netherlands. *First Break*, 37(7):57–66, 2019.

[20] BNEF. Hydrogen: The Economics of Storage. Technical report, BNEF, 2019.

[21] Viktor Reitenbach, Leonhard Ganzer, Daniel Albrecht, and Birger Hagemann. Influence of added hydrogen on underground gas storage: a review of key issues.

[22] Christina Hemme and Wolfgang van Berk. Hydrogeochemical modeling to identify potential risks of underground hydrogen storage in depleted gas fields. *Applied Sciences (Switzerland)*, 8(11), nov 2018.

[23] Thijs Verboon Bert den Ouden, John Kerkhoven, Jan WarnaarsRob Terwel, Max Coenen and Tuuli Tiihonen & Anne Koot. Klimaatneutrale energiescenario's 2050. Technical report, Berenschot & Kalavasta, 2020.

[24] Gruber. Shimko M.A., Parkster M. Combined Reverse-Brayton Joule Thompson Hydrogen Liquification Cycle, 2005.

[25] ILK Dresden. "Storage Density of Hydrogen under certain pressure and temperature conditions".

[26] J. Rutqvist. The geomechanics of CO2 storage in deep sedimentary formations. Technical report, Geotech. Geol. Eng, 2012.

[27] Victor Vilarrasa, · Diogo, Marco Dentz, Sebastia Olivella, Jesus Carrera, and Diogo Bolster. Effects of CO 2 Compressibility on CO 2 Storage in Deep Saline Aquifers. Technical report.

[28] Hydrogen Properties - Hydrogen Tools.

[29] Azaroual M. Lassin A., Dymitrowska M. " Hydrogen solubility in pore water of partially saturated argillites: Application to Callovo-Oxfordian clayrock in the context of a nuclear waste geological disposal". Technical report, Elesvier Ltd, 2011.

[30] M. P. Pichler. Assesment of hydrogen rock interaction during geological storage of CH4-H2 mixtures. *Sustainable Earth Sciences, SES 2013: Technologies for Sustainable Use of the Deep Sub-Surface*, 2013.

[31] Minnich B.H. Pray H.A., Schweickert C.E. " Solubility of Hydrogen, Oxygen, Nitrogen Institute, and Helium in Water: At elevated temperatures.". Technical report, Battelle Memorial, Ohio, 1950.

[32] P O Carden and L Paterson. PHYSICAL, CHEMICAL AND ENERGY ASPECTS OF UNDERGROUND HYDROGEN STORAGE. Technical report.

[33] F. Feldmann, B. Hagemann, L. Ganzer, and M. Panfilov. Numerical simulation of hydrodynamic and gas mixing processes in underground hydrogen storages. *Environmental Earth Sciences*, 75(16), aug 2016.

[34] Perminc. "Miscible Displacement Fluid Properties in Miscible Displacement: Macroscopic Displacement Efficiency," . Available: .

[35] L.W. Lake. *Enhanced Oil Recovery*. Prentice-Hall, Englewood Cliffs, 1989.

[36] Marco Dentz and Daniel M Tartakovsky. Abrupt-Interface Solution for Carbon Dioxide Injection into Porous Media. *Transp Porous Med*, 79:15–27, 2009.

[37] H. Hajibeygi. AESM1325 Physics For Geosystems - Dispersion, 2019.

[38] B. Hagemann, M. Rasoulzadeh, M. Panfilov, L. Ganzer, and V. Reitenbach. Mathematical modeling of unstable transport in underground hydrogen storage. *Environmental Earth Sciences*, 73(11):6891–6898, jun 2015.

[39] H. Hajibeygi. AES1350 Reservoir Simulation, 2019.

[40] H. Hajibeygi and D Voskov. DARSim, 2020.

[41] Nitrogen - Thermophysical Properties.

[42] Wolf Tilmann Pfeiffer and Sebastian Bauer. Subsurface Porous Media Hydrogen Storage - Scenario Development and Simulation. In *Energy Procedia*, volume 76, pages 565–572. Elsevier Ltd, 2015.

[43] Balaji S Srinivasan. The impact of reservoir properties on mixing of inert cushion and The impact of reservoir properties on mixing of inert cushion and natural gas in storage reservoirs natural gas in storage reservoirs. Technical report.

A

Need for seasonal H_2 storage in Klimaatneutrale Energiescenario's 2050

Regional Management	National Management	European Management	International Management
The Netherlands achieves CO2 reduction targets due to regional managent	The Netherlands achieves CO2 reduction targets as frontrunner in Europe	Europe achieves CO2 reduction targets as international frontrunner	Drastic reduction in global usage of fossil fuels
100% CO_2-reducton achieved in The Netherlands	100% CO_2-reducton achieved in The Netherlands	100% CO_2-reducton achieved in Europe	Worldwide 100% CO_2-reducton achieved
Fully autonomous energy system	High degree of autononmous energy system	European CO_2 ad import taxes on energy	Free trade of energy is stimulated
Geen importen van energie	Minimale importen van energie	Wereldwijde waterstofmarkt	Wereldwijde waterstofmarkt
Decrease of energy-intensive industry	Scale of energy-intensive industry remains the same	Growth of energy-intensive industry	Growth of energy-intensive industry

Figure A.0.1: Detailed overview of key assumptions in the different climate-neutral scenarios described by Berenschot & Kalavasta [23]

An overview of the main assumptions that are made in each of the climate-neutral management scenarios described by *Berenschot & Kalavasta* [23]. The National Management scenario showed to have the lowest need for seasonal storage of H_2. The highest need of H_2 storage was identified using the International Management scenario primarily due to the need for strategical H_2 storage.

B

Selection of Offshore Reservoirs from the Main Buntsandstein Unit in The Netherlands

	Units	fraction	fraction	fraction	fraction
FIELD$_{CD}$	STRAT$_{UNIT_NM}$	MIN$_P$*OROSITY*	MAX$_P$*OROSITY*	AVG$_P$*OROSITY*	MIN$_C$*ORE$_P$OROSITY*
P06-D	Main Buntsandstein Subgroup				0.013
P06-D	Z3 Carbonate Member				0.008
P06-Main	Main Buntsandstein Subgroup	0.08	0.08	0.08	0.001
P06-Main	Slochteren Formation				0.017
P06-Main	Z3 Carbonate Member	0.027	0.027	0.027	0.002
P06 NW	Main Buntsandstein Subgroup				0.011
P06 NW	Z3 Carbonate Member				0.001
P06-S	Main Buntsandstein Subgroup	0.087	0.087	0.087	0.026
P06-S	Zechstein Group	0.087	0.087	0.087	0.014
P09-A	Solling Formation	0.081	0.081	0.081	0.007
P09-B	Solling Formation	0.098	0.098	0.098	
P15-10	Main Buntsandstein Subgroup	0.123	0.123	0.123	0.086
P12-SW	Main Buntsandstein Subgroup	0.107	0.107	0.107	0
P15-11	**Main Buntsandstein Subgroup**	**0.127**	**0.127**	**0.127**	**0.039**
P15-14	Main Buntsandstein Subgroup	0.15	0.15	0.15	0.016
P18-2	Main Buntsandstein Subgroup				
P18-2	Main Buntsandstein Subgroup	0.12	0.14	0.13	0.021
P18-2	Main Buntsandstein Subgroup	0.08	0.08	0.08	
P18-2	Main Buntsandstein Subgroup				0.031
Q01-B	Main Buntsandstein Subgroup				0.038
Q01D	Main Buntsandstein Subgroup				0.012
Q01-NW	Vlieland Sandstone Formation				0.165

		Units	fraction	fraction	fraction	fraction	
FIELD$_C D$	STRAT$_U NIT_N M$	MAX$_C ORE_P OROSITY$	AVG$_C ORE_P OROSITY$	MIN$_C ORE_H ORPERM$	MAX$_C ORE_H ORPERM$	AVG$_C ORE_H ORPERM$	
P06-D	Main Buntsandstein Subgroup	0.219	0.096	0.01	3142.01	41.347	
P06-D	Z3 Carbonate Member	0.057	0.027	0.01	8.51	1.812	
P06-Main	Main Buntsandstein Subgroup	0.171	0.079	0.009	2100	6.362	
P06-Main	Slochteren Formation	0.167	0.127	0.01	2.3	0.165	
P06-Main	Z3 Carbonate Member	0.184	0.036	0.01	338	12.301	
P06 NW	Main Buntsandstein Subgroup	0.168	0.076	0.01	95	1.667	
P06 NW	Z3 Carbonate Member	0.091	0.014	0.01	11	1.056	
P06-S	Main Buntsandstein Subgroup	0.128	0.082	0.05	4.6	0.809	
P06-S	Zechstein Group	0.05	0.029	0.09	7.9	1.89	
P09-A	Solling Formation	0.131	0.068	0.01	143.26	11.126	
P09-B	Solling Formation						
P15-10	Main Buntsandstein Subgroup	0.173	0.124	2.9	529	119.121	
P12-SW	Main Buntsandstein Subgroup	0.213	0.083	0.01	414	9.731	
P15-11	**Main Buntsandstein Subgroup**	**0.241**	**0.141**	**0.07**	**3200**	**283**	
P15-14	Main Buntsandstein Subgroup	0.178	0.103	0.032	183	86.69	
P18-2	Main Buntsandstein Subgroup						
P18-2	Main Buntsandstein Subgroup	0.231	0.091	0.01	3000	76.709	
P18-2	Main Buntsandstein Subgroup						
P18-2	Main Buntsandstein Subgroup	0.231	0.095	0.01	3000	135.936	
Q01-B	Main Buntsandstein Subgroup	0.307	0.156	0.01	16201	421.247	
Q01D	Main Buntsandstein Subgroup	0.179	0.081	0	116	5.719	
Q01-NW	Vlieland Sandstone Formation	0.269	0.251	164.75	1264.84	672.409	

	Units	deg. Celcius	
FIELD$_C D$	STRAT$_U NIT_N M$	MAX$_I NIT_T EMP$	AVG$_P OROSITY$
P06-D	Main Buntsandstein Subgroup		
P06-D	Z3 Carbonate Member		
P06-Main	Main Buntsandstein Subgroup		0.08
P06-Main	Slochteren Formation		
P06-Main	Z3 Carbonate Member	111.1	0.027
P06 NW	Main Buntsandstein Subgroup		
P06 NW	Z3 Carbonate Member		
P06-S	Main Buntsandstein Subgroup	121	0.087
P06-S	Zechstein Group	121	0.087
P09-A	Solling Formation		0.081
P09-B	Solling Formation		0.098
P15-10	Main Buntsandstein Subgroup	90	0.123
P12-SW	Main Buntsandstein Subgroup	91.5	0.107
P15-11	**Main Buntsandstein Subgroup**	**102**	**0.127**
P15-14	Main Buntsandstein Subgroup		0.15
P18-2	Main Buntsandstein Subgroup		
P18-2	Main Buntsandstein Subgroup	114.4	0.13
P18-2	Main Buntsandstein Subgroup	114.4	0.08
P18-2	Main Buntsandstein Subgroup		
Q01-B	Main Buntsandstein Subgroup		
Q01D	Main Buntsandstein Subgroup	110	
Q01-NW	Vlieland Sandstone Formation		

C

Gravity Number Analysis

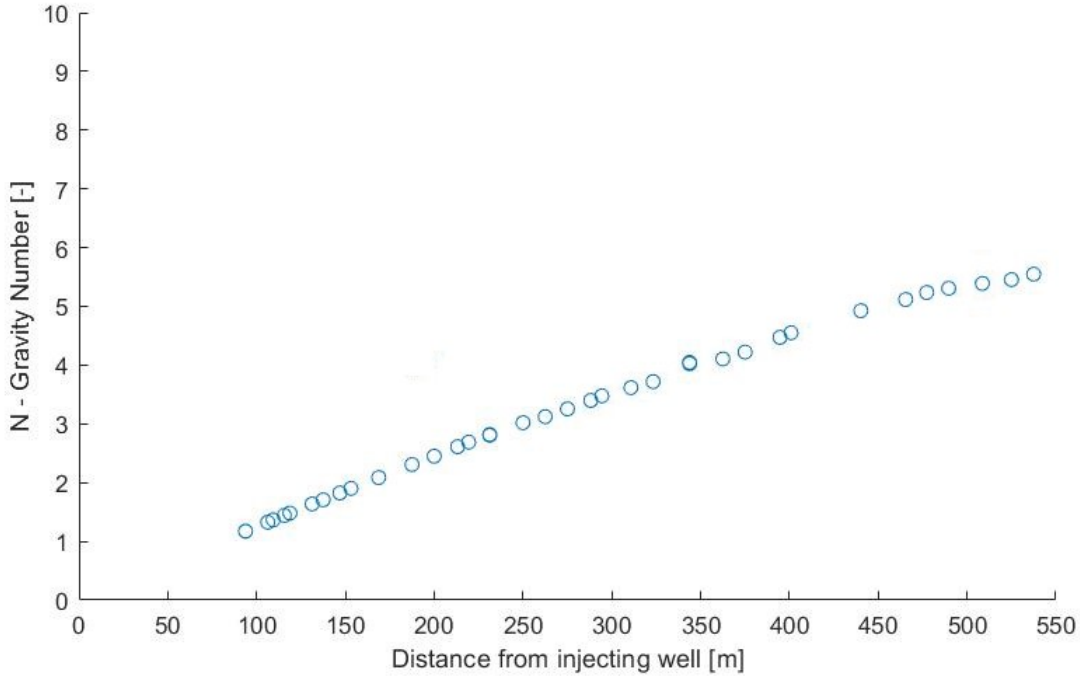

Figure C.0.1: Gravity Number N as a function of distance from the injecting well

In Figure C.0.1 the value for the dimensionless gravity number N as a function of the characteristic distance r_c is visualized. Noticeable is the roughly linear increase in gravity number the further the distance is from the injection wells. Therefore, in proximity of the injection well, a comparable ratio between the gravitational and viscous forces is seen. The more we move away from the well, the more the gravitational forces will dominate.

D

Delft Sandstone Reservoir

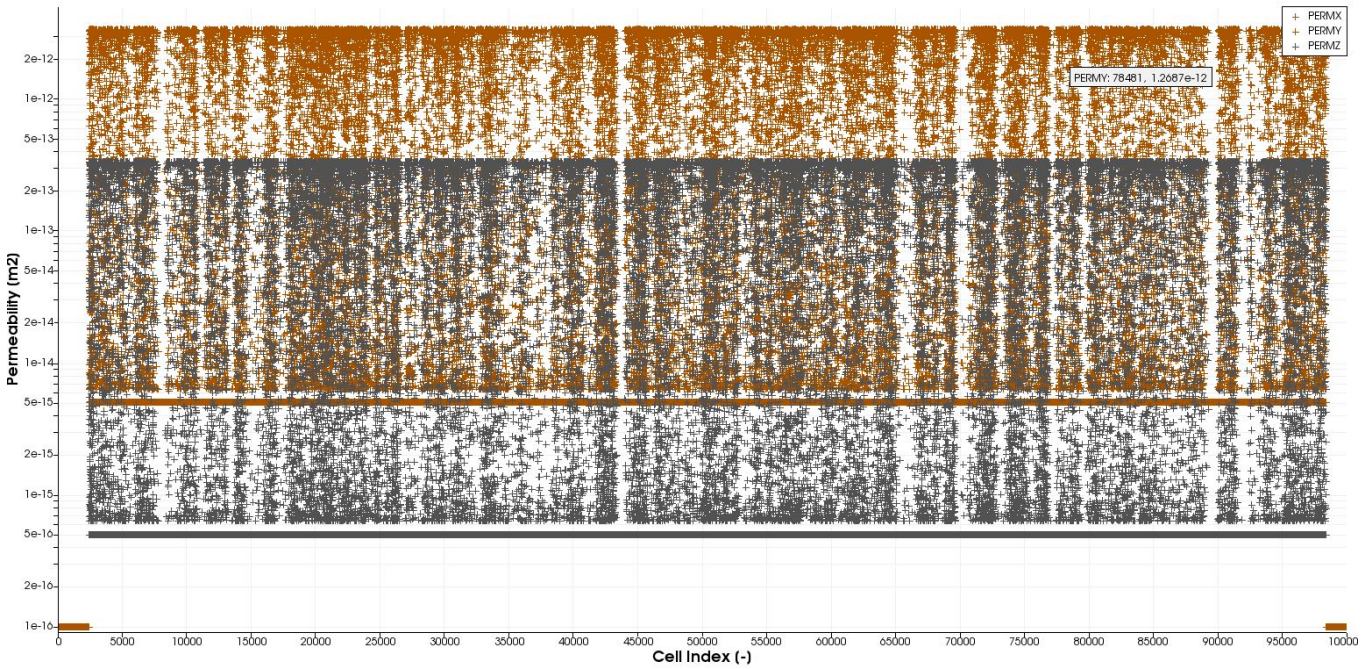

Figure D.0.1: Full Permeability Distribution of the Delft Sandstone

In Figure D.0.1, the full distribution of the permeability values are visualized. Noticeable is the very low permeability of $1 \cdot 10^{-16}\ m^2$in the caprock. Furthermore, the low horizontal permeable zones are respectively $5 \cdot 10^{-15}\ m^2$ for $K_{xy}$and $5 \cdot 10^{-16}\ m^2$ for K_z.

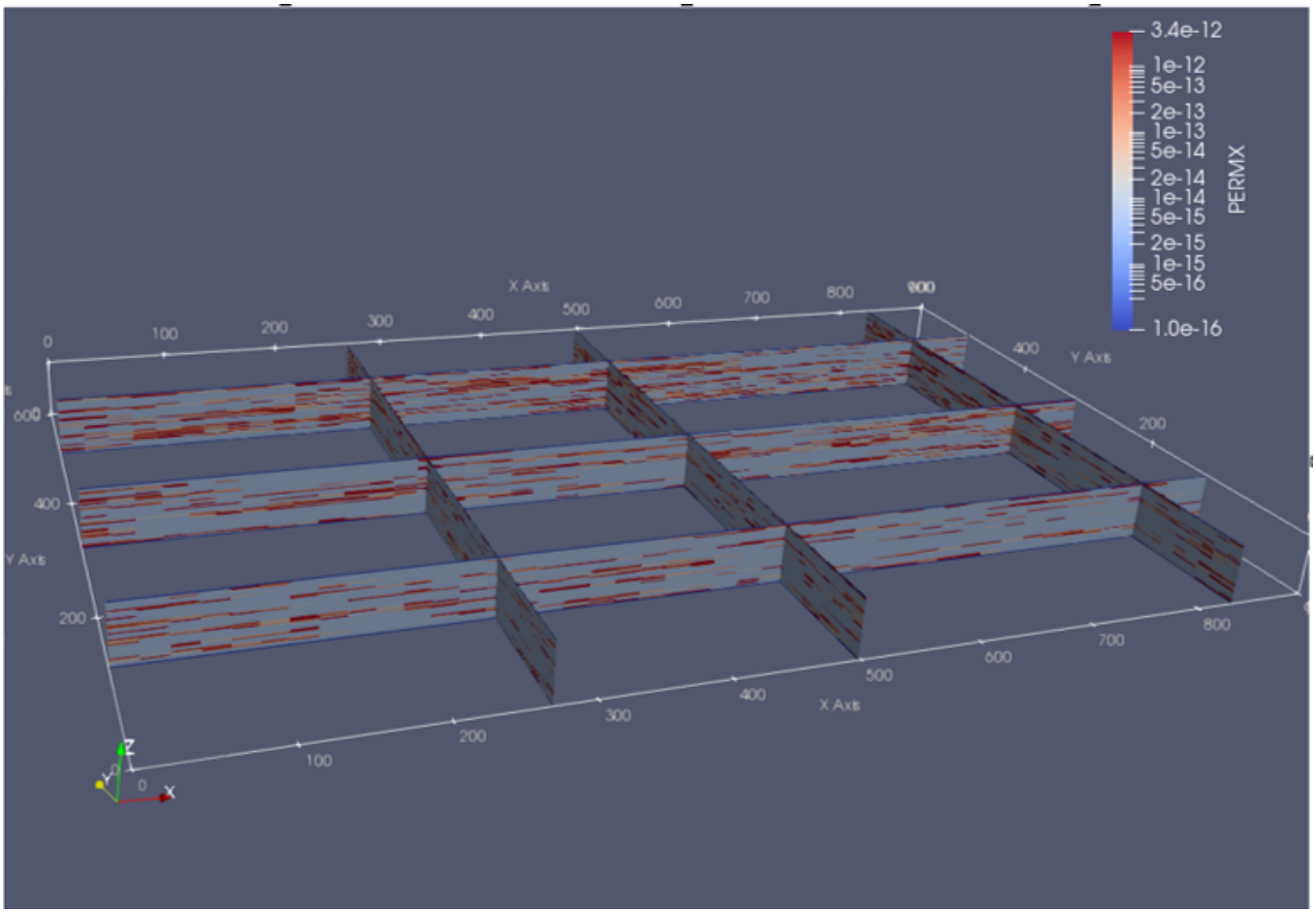

Figure D.0.2: 3 Dimensional view of the Delft Sandstone Dataset

E

2D slices of 3D Cyclic Simulations

In the following figures is the concentration of H_2 in the reservoir visualized throughout different time steps during the cyclic storage of H_2 in the homogeneous reservoir. These figures make it clear where the irretrievable H_2 is located in the reservoir.

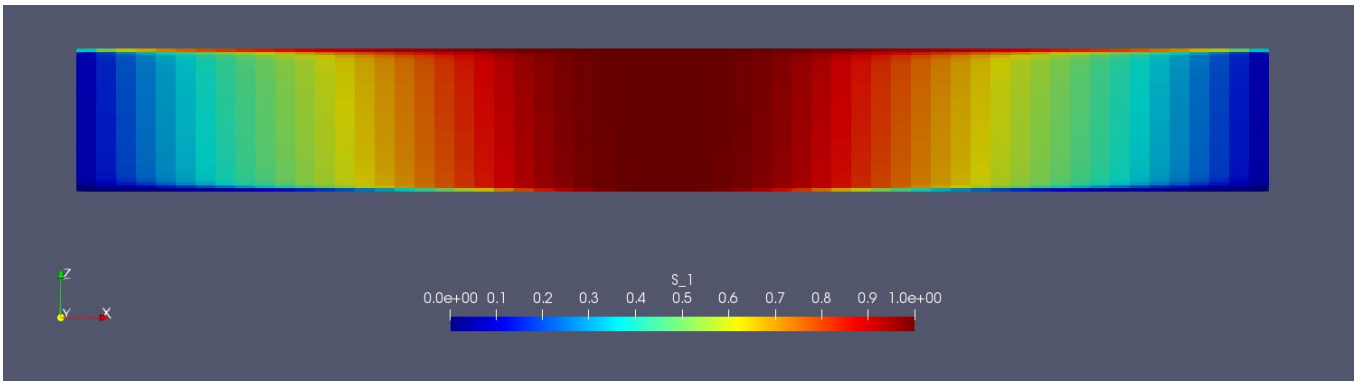

Figure E.0.1: Concentration of H_2 in reservoir at the end of injection cycle 1

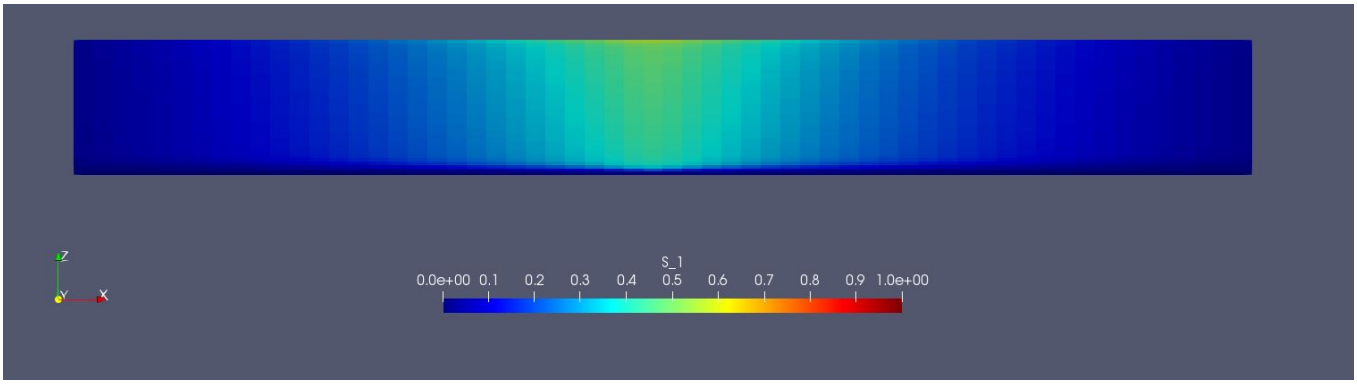

Figure E.0.2: Concentration of H_2 in reservoir at the end of production cycle 1

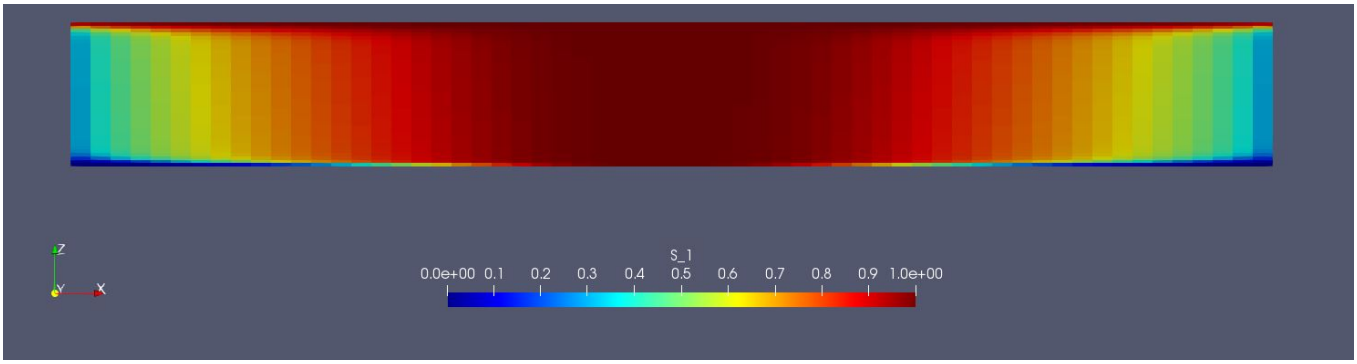

Figure E.0.3: Concentration of H_2 in reservoir at the end of injection cycle 2

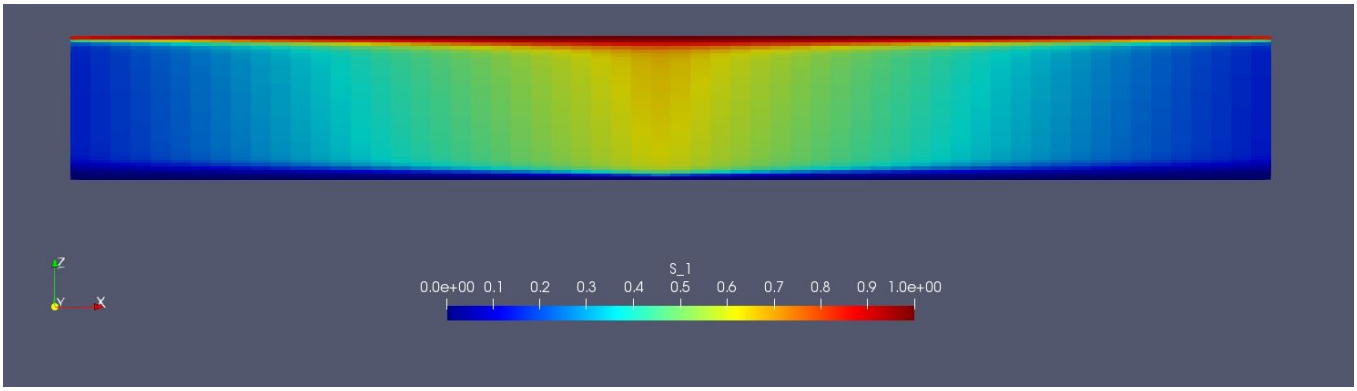

Figure E.0.4: Concentration of H_2 in reservoir at the end of production cycle 2

F

Sensitivity Analysis

This section shows the upper an lower pressure constraints used to analyze the sesntivity of the injection and production stages.

F.1. Increased Net Pressure Difference - Scenario A

Stage 1 (Injection)	Value	Unit
P_{init}	30	Bar
P_{inj}	170	Bar
P_{prod}	-	Bar

Stage 2 (Production)	Value	Unit
P_{ini}	170	Bar
P_{inj}	-	Bar
P_{prod}	30	Bar

Stage 3 (H_2 Injection)	Value	Unit
P_{ini}	30	Bar
P_{inj}	170	Bar
P_{prod}	-	Bar

Stage 4 (H_2 Production)	Value	Unit
P_{ini}	170	Bar
P_{inj}	-	Bar
P_{prod}	30	Bar

Table F.1.1: Scenario A

F.2. Decreased Net Pressure Difference - Scenario B

Stage 1 (Injection)	Value	Unit
P_{init}	30	Bar
P_{inj}	65	Bar
P_{prod}	-	Bar

Stage 2 (Production)	Value	Unit
P_{ini}	65	Bar
P_{inj}	-	Bar
P_{prod}	30	Bar

Stage 3 (H_2 Injection)	Value	Unit
P_{ini}	30	Bar
P_{inj}	65	Bar
P_{prod}	-	Bar

Stage 4 (H_2 Production)	Value	Unit
P_{ini}	65	Bar
P_{inj}	-	Bar
P_{prod}	30	Bar

Table F.2.1: Scenario B